Molecular thermodynamics for amino-acid adsorption at inorganic surfaces

Journal:	*AIChE Journal*
Manuscript ID	AIChE-21-23814.R1
Wiley - Manuscript type:	Research Article
Date Submitted by the Author:	n/a
Complete List of Authors:	Gallegos, Alex Wu, Jianzhong; University of California, Riverside, Department of Chemical Engineering and Environmental Engineering
Keywords:	Interfacial processes, Adsorption/liquid, Thermodynamics/statistical, Surface chemistry/physics

Molecular thermodynamics for amino-acid adsorption at inorganic surfaces

Alejandro Gallegos and Jianzhong Wu*

Department of Chemical and Environmental Engineering, University of California, Riverside, CA 92521, USA

Abstract

The interaction of polypeptides and proteins with an inorganic surface is intrinsically dependent on the interfacial behavior of amino acids and sensitive to solution conditions such as pH, ion type, and salt concentration. A faithful description of amino-acid adsorption remains a theoretical challenge from a molecular perspective due to the strong coupling of local thermodynamic nonideality and inhomogeneous ionization of both the adsorbate and substrate. Building upon a recently developed coarse-grained model for natural amino acids in bulk electrolyte solutions, here we report a molecular theory to predict amino-acid adsorption on ionizable inorganic surfaces over a broad range of solution conditions. In addition to describing the coupled ionization of amino acids and the underlying surface, the thermodynamic model is able to account for both physical binding and surface associations such as hydrogen bonding or bidentate coordination. It is applicable to all types of natural amino acids regardless of the solution pH, salt type and concentration. The theoretical predictions have been validated by extensive comparison with experimental data for the adsorption of acidic, basic, and neutral amino acids at rutile (α-TiO_2) surfaces.

Keywords:

Surface adhesion, charge regulation, classical density functional theory

* Corresponding author. E-mail addresses: jwu@engr.ucr.edu

1. Introduction

Understanding the interaction of amino acids with inorganic surfaces is a prerequisite for studying the interfacial behavior of polypeptides and proteins under various solution conditions. By reducing the complexity of the polymeric systems to their building blocks, we may identify key components of surface forces dictating both the adsorption and functionality of biomolecules at the interface[1-3]. However, despite its simplicity in comparison with proteins, the adsorption of amino acids in aqueous solutions is not yet fully understood from a molecular perspective[4]. The difficulty arises not only from multifaceted interactions between amino acids and an inorganic surface but also from the variation of both the surface charge and the degree of ionization of the functional groups in response to the changes in solution conditions such as pH, ion type, and salt concentration.

In addition to amine and carboxyl groups, natural amino acids consist of different side chains that vary in size and hydrophobicity. The diverse characteristics of these functional groups leads to complex interactions with inorganic surfaces in an aqueous medium. Conventionally, the surface forces are described in terms of electrostatic interactions, van der Waals and hydrophobic attractions, hydration forces, and various forms of surface association or chemical bonding. The intricate interplay of these physical and chemical interactions is coupled with protonation/deportation and multi-body correlations due to the inhomogeneous distributions of ionic species (and solvent molecules) near the surface. For most systems of practical interest, a first principles approach to predicting such interactions is beyond the reach of current computation capabilities. As a result, coarse-grained models may serve as a reasonable starting point to describe the adsorption and surface behavior.

A number of experimental techniques can be used to study the adsorption of amino acids at inorganic surfaces[5-8]. One such technique is infrared (IR) spectroscopy, which provides valuable insight into the mechanisms of amino-acid adsorption through the comparison of the spectra of adsorbed species versus that in the bulk solution. For example, IR measurements revealed glutamic acid and aspartic acid binding with γ-Al_2O_3 through oxygen atoms from one or both carboxyl groups[9]. An indirect way to measure amino-acid adsorption is by monitoring its concentration in the bulk phase[7,10-13]. The adsorption isotherm, i.e., the amount of amino acid adsorbed on the surface as a function of the *equilibrium* concentration in the bulk solution, can be determined from the reduction of the amino-acid concentration in the bulk solution. Radiotracer experiments are applicable to adsorption from dilute solutions whereby the depletion method is not possible[14]. With the help of a semi-empirical model such as the Langmuir equation, the adsorption isotherms provide valuable insight into the strength of surface binding and the maximum occupancy of amino acids. Whereas conventional adsorption models may be employed as a benchmark to compare the adsorption of amino acids at different surfaces, the model parameters are typically dependent on solution conditions thus have little predictive capability.

Complementary to experimental investigations, molecular modeling offers valuable details to bridge the knowledge gap between microscopic and macroscopic observations. Whereas atomistic models can be used to describe amino-acid adsorption through molecular dynamics (MD) simulation[15-17], coarse-grained models are often more convenient for the development of analytical methods. By capturing the essential features of intermolecular interactions and surface forces, coarse-grained models are able to provide quantitative predictions in good agreement with experimental observations. For example, Vlasova and Golovkova studied the adsorption of basic amino acids to highly dispersed silica using a surface-complexation model that describes the

amino-acid molecules at the silica surface through a Stern model of the electric double layer[18]. Two parameters were used for each amino acid, *viz*., the equilibrium constants governing the reaction of amino acids with a neutral or a negatively charged surface. With the assumption that these parameters were dependent upon the salt concentration but insensitive to the pH, the theoretical predictions of adsorption isotherms were found in quantitative agreement with experimental data. Similarly, Jonsson et al. proposed a surface-complexation model to describe the adsorption isotherms of L-aspartate and L-glutamate to a rutile surface at various solution conditions[19,20]. They proposed a reaction scheme that involved association of the acidic amino acids with the rutile surface through the binding of either one or both carboxyl groups to one or four surface titanium sites, respectively. Like the Langmuir adsorption isotherm, the surface-complexation models neglect thermodynamic non-ideality due to excluded volume effects and electrostatic correlations that are important in describing the charge regulation of amino acids both in the bulk solution and near the surface.

In order to accurately describe the adsorption of amino acids to inorganic surfaces, we must account for thermodynamic non-ideality due to interactions between amino acids and all ionic species in the solution. In addition, it is essential to capture the charge behavior of amino acids as well as the ionization of the inorganic surfaces that play a significant role in the adsorption process. In our previous work, we developed a coarse-grained model for aqueous solutions of amino acids that appropriately takes into account bulk interactions[21]. The thermodynamic model provides a faithful description of the charge behavior of amino acids as a function of pH and solution conditions. In addition, we proposed a coarse-grained model to describe the charge regulation of various ionizable surfaces by an explicit consideration of the inhomogeneous ion distributions and surface reactions[22-24]. Herein, we combine these models to examine the adsorption behavior of

amino acids at the rutile (α-TiO_2) surface. The molecular-thermodynamic model allows us to predict the adsorption of various amino acids in response to the changes in solution conditions. This predictive model fills the gap between phenomenological models to describe the adsorption of amino acids and all-atom or first-principles simulations. Importantly, the theoretical procedure may provide a foundation for future studies of the interaction of polypeptides and proteins with various inorganic surfaces under diverse solution conditions.

2. Thermodynamic Model and Methods

2.1 *A coarse-grained model for amino-acid adsorption*

In this work, we are interested in developing a coarse-grained model applicable to amino-acid adsorption at an ionizable surface over a broad range of solution conditions. Toward that end, we employ an augmented primitive model (APM) that explicitly accounts for the different charged states of natural amino acids[21]. Due to the variation of hydration structure in response to the deprotonation or protonation of ionizable sites, each amino-acid molecule has a unique hard-sphere diameter σ_i and valence Z_i in different charged states.

Figure 1 shows a schematic representation of amino acids near an organic surface as described by the APM model. As in the primitive model (PM) that is conventionally used to describe the thermodynamic properties of aqueous electrolyte solutions, all amino acids and ionic species are represented by charged hard spheres and the solvent by a dielectric continuum of relative primitivity $\varepsilon_r = 78$, which corresponds to that for liquid water at the ambient condition. Because of ionization, each amino acid exists as a mixture of molecules in discrete integer-value charge states. In addition to the variation of the valence in response to pH changes, the augmented aspect of the primitive model is the inclusion of various well-recognized but poorly-understood water-mediated interactions among amino acids and other ionic species in the solution as well as

their short-range interactions with the surface. In this work, such interactions are described through a square-well model. While the phenomenological description neglects atomic details and the anisotropic nature of amino-acid molecules, it provides a flexible framework to quantify the interfacial behavior of various natural amino acids in aqueous solutions by treating the square-well width and attraction energy as adjustable parameters. We demonstrated in our previous work that the augmented model is able to reproduce both the titration behavior and the thermodynamic properties of amino-acid solutions in good agreement with experimental observations[21].

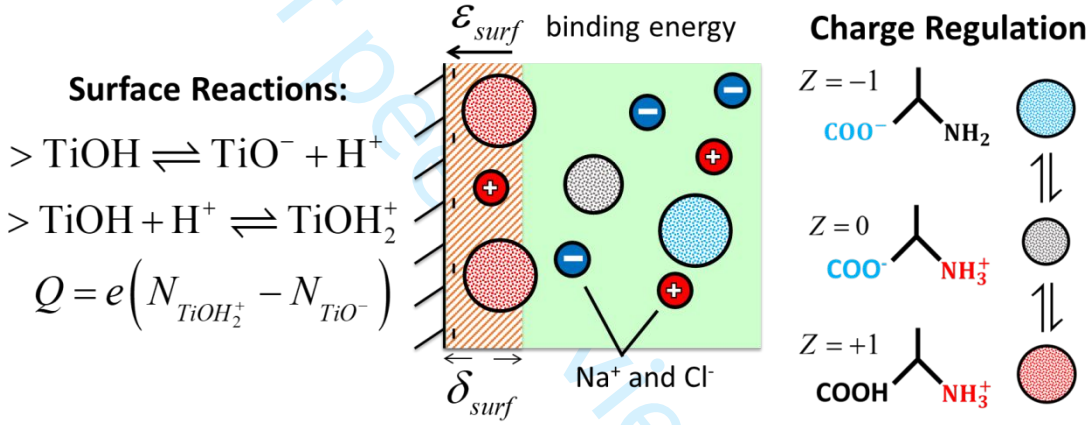

Figure 1. A coarse-grained model for the adsorption of natural amino acids on a rutile surface. In an aqueous solution, an amino-acid molecule may exist in different charged states dependent on the solution condition. The rutile surface may develop a net charge through deprotonation or protonation of the hydroxyl sites.

The coarse-grained model can be similarly applied to the adsorption of amino acids at an inorganic surface. In this case, the surface is represented by a hard wall with the charge density determined from the dissociation equilibrium of ionizable sites and ionic distributions self-consistently[22-24]. In addition to the electrostatic interactions and excluded volume effects, the surface interacts with amino acids through semi-empirical short-range interactions (e.g., hydrophobic attraction and hydrogen bonding). As in the PM description of electrolyte solutions,

the van der Waals attraction is relatively insignificant in comparison with other forms of surface forces. Because our model accounts for ionization and the electrostatic charges of amino-acid molecules explicitly, we neglect the polarity effects on intermolecular and surface interactions. Our results suggest that the remanent electrostatic effects are effectively accounted for by short-range bindings. For simplicity, we fix the range of the short-range interaction between the surface and all amino acids at δ_{surf} = 0.4 nm from the edge of the hard wall (see Figure 1). The choice of four angstroms is somewhat arbitrary in that a shift of the range of attraction can always be compensated by changing the energy parameter. Nevertheless, the chosen value appears reasonable from physical considerations because both hydrophobic interactions and hydrogen bonding are most significant when the amino acid is in intimate contact with the surface. It should be noted that δ_{surf} is immaterial to the identity of amino acids.

According to APM, the external potential due to the inorganic surface is expressed as

$$V_i^{ext}(z) = \begin{cases} \infty & z < \sigma_i / 2 \\ -\varepsilon_{surf,i} & \sigma_i / 2 \le z \le \delta_{surf} \\ 0 & else \end{cases} . \quad (1)$$

In Eq. (1), the first line on the right accounts for the hard-wall repulsion, which limits the access of a chemical species (viz., ions and amino acids) to the solid phase beyond the point of contact; and the second line accounts for the short-range attraction. The latter is represented by a square-well potential with a constant energy in the immediate vicinity of the surface. Because of the excluded-volume effects, the closest distance for an amino acid from the surface depends on its hard-sphere diameter. As a result, the range of non-electrostatic surface attraction is different for different amino acids. On the other hand, the square-well energy, ε_{surf}, accounts for specific binding of an amino acid molecule with the surface. We expect that this parameter should be

relatively insensitive to the changes in solution conditions (e.g., salt concentration), but may vary with temperature, because it reflects the local properties of the underlying chemical species. The results here are reported for T=298.15 K. The surface energy may also be used to account for adsorption of amino acids due to specific chemical bonding with the surface. To a certain degree, our description of amino-acid binding with an inorganic surface is equivalent to surface complexation modeling mentioned above[25,26]. One benefit of our thermodynamic approach is that it takes into account the solution effects on amino-acid adsorption.

2.2 *Charge regulation for inorganic surfaces*

In an aqueous solution, inorganic surfaces are typically terminated with hydroxyl groups due to the chemical adsorption of water molecules[27]. The deprotonation or protonation of these functional groups leads to a surface charge that can be regulated by adjusting the solution pH or salt concentration. Even for the same surface, the charge density may differ in both magnitude and sign depending on the solution conditions.

Due to its broad use as bioimplants, titanium dioxide is commonly used as a model inorganic material for studying amino-acid adsorption. In particular, experimental studies are mostly focused on rutile (100) and (110) surfaces as single crystals with these orientations are readily available. For a rutile surface, the deprotonation and protonation reactions are given by[28]

$$\text{-TiOH} \rightarrow \text{-TiO}^- + \text{H}^+, \tag{2}$$

$$\text{-TiOH} + \text{H}^+ \rightarrow \text{-TiOH}_2^+. \tag{3}$$

The equilibrium constants for these two reactions, K_D and K_P, respectively, are connected with the solution $\text{pH} = -\log a_{H^+}$ and the activities of the surface sites:

$$K_D = \frac{N_{TiO^-}}{N_{TiOH}} \frac{\gamma_{TiO^-}}{\gamma_{TiOH}} a_{H^+}, \tag{4}$$

$$K_P = \frac{N_{TiOH_2^+}}{N_{TiOH}} \frac{\gamma_{TiOH_2^+}}{\gamma_{TiOH}} \frac{1}{a_{H^+}} \tag{5}$$

where N_i refers to the number of surface site *i* per unit area, and γ_i is the activity coefficient of the corresponding surface site.

The activity coefficient of each surface group accounts for its physical interactions with the environment[29]. In this work, we assume that the ratio of the activity coefficients for each surface group in its different charge states to be governed by the local electrostatic potential (i.e., the surface potential, ψ_s). Thus, the surface reaction equilibrium can be re-expressed in terms of apparent equilibrium constants, K_D' and K_P',

$$K_D' = K_D \frac{\gamma_{SOH}}{\gamma_{SO^-}} = K_D \exp\left(\beta e \psi_s\right), \tag{6}$$

$$K_P' = K_P \frac{\gamma_{SOH}}{\gamma_{SOH_2^+}} = K_P \exp\left(-\beta e \psi_s\right). \tag{7}$$

The surface charge density is related to the total number density of the site and can be determined from the mass and charge balance:

$$N_{sites} = N_{SOH} + N_{SO^-} + N_{SOH_2^+}, \tag{8}$$

$$Q = -e\left(N_{SO^-} - N_{SOH_2^+}\right) \tag{9}$$

where N_{sites} refers to the total number of surface groups per unit area, *e* is the elementary charge, and Q is the surface charge density.

The combination of Eqs. (4-9) leads to an explicit expression for the surface charge density in terms of the total number of available sites per unit area, the apparent equilibrium constants, and the proton activity:

$$Q = -e\,N_{sites}\frac{K_D'/a_{H^+} - K_P' a_{H^+}}{1 + K_D'/a_{H^+} + K_P' a_{H^+}}. \tag{10}$$

Since the apparent equilibrium constants change with the surface potential, the surface charge density depends on the inhomogeneous ion distributions near the surface. As a result, the charge regulation of amino acids is more complex than that in the bulk solution due to the interfacial behavior of all charged species playing a key role in determining the local solution condition.

2.3 ***Ionization of amino acids in an inhomogeneous environment***

Each amino acid molecule consists of a carboxyl group and an amine group which can be deprotonated and protonated, respectively, at suitable solution conditions. Neutral amino acids are referred to as those that do not contain any ionizable functional groups in the side chain. On the other hand, acidic and basic amino acids contain an additional functional group in their side chains that can be deprotonated and protonated, leading to an additional negative and positive charge, respectively. As a result of the acid-base equilibrium, amino acids exist in multiple charged states dependent on the pH and other solution conditions.

For each amino acid, the acid-base equilibrium can be described in terms of multi-step protonation reactions

$$\mathrm{A_{i-1}} + \mathrm{H^+} \leftrightarrow \mathrm{A_i} \tag{11}$$

where $\mathrm{A_i}$ refers to the amino acid in a given charged state. The amino-acid valence satisfies $Z_{A_i} = Z_{A_0} + i$ with $Z_{\mathrm{A_0}}$ being the charge for the amino acid in its fully deprotonated state. For a neutral or basic amino acid, $Z_{\mathrm{A_0}} = -1$; while an acidic amino acid has a valence of -2 in its fully deprotonated state. Accordingly, in the fully protonated state, each neutral or acidic amino acid has a valence of +1, and each basic amino acid has a valence of +2.

Similar to that in the bulk solution, the equilibrium constant for the protonation of amino acids in an inhomogeneous environment (viz., near the surface) is related to the local solution composition and activity coefficients

$$K_i^T = \frac{\rho_{A_i}(z)}{\rho_{A_{i-1}}(z)} \frac{\gamma_{A_i}(z)}{\gamma_{A_{i-1}}(z)} \frac{1}{a_{H^+}} \tag{12}$$

where K_i^T represents the equilibrium constant for the amino acid in charge state i, $\rho_i(z)$ is the number density of species i at perpendicular distance z from the surface, and γ_i is its local activity coefficient. The equilibrium constant is a thermodynamic quantity defined by the change in the chemical potentials of reactants and products at their corresponding reference states, i.e., each species in an ideal solution at unit molar concentration[30]. These values were obtained in our previous work based off correlations with experimental data for all natural amino acids in bulk NaCl solutions[21]. The activity coefficients account for the effect of solvent-mediated interactions among all chemical species in the solution.

Within the augmented primitive model (APM), the local activity coefficient can be expressed as

$$k_B T \ln \gamma_i = \mu_i^{ex} = \mu_i^{hs} + \mu_i^{sw} + \mu_i^{el} + \psi Z_i e + V_i^{ext} \tag{13}$$

where μ_i^{ex} stands for the local excess chemical potential, *i.e.*, deviation from the chemical potential of species i in an ideal solution; k_B is the Boltzmann constant, and T is the absolute temperature. μ_i^{hs}, μ_i^{el}, and μ_i^{sw} are contributions to the local excess chemical potential due to hard-sphere repulsion, electrostatic correlation, and solvent-mediated interactions, respectively. The last two terms, V_i^{ext} and ψ, are the external potential due to the interface (e.g., hard wall and specific

binding to the surface) and the local electrostatic potential, respectively. The expression for each contribution has been discussed previously and can be found in Supporting Information[31-33].

2.4 *Classical Density Functional Theory*

Classical density functional theory (cDFT) provides a generic mathematical procedure to describe the inhomogeneous distributions of ionic species including amino acids near inorganic surfaces. At a given temperature T and the bulk densities of all ionic species $\{\rho_i^b\}$, cDFT predicts the local density, $\rho_i(z)$, of each species by minimizing the grand potential

$$\Omega = F + \sum_i \int \left[V_i^{ext}(z') - \mu_i \right] \rho_i(z') dz' \tag{14}$$

where V_i^{ext} and μ_i are the external potential and the chemical potential of species i, respectively, and F denotes the total intrinsic Helmholtz energy. The latter consists of an ideal-gas contribution and the excess arising from intermolecular interactions. Similarly, the chemical potential is composed of an ideal part, which is directly related to the number density of the species, and an excess part as discussed in the prior section.

For systems considered in this work, the intermolecular interactions include the hard-sphere repulsion, electrostatic correlations, solvent-mediated interactions, and direct coulombic interactions. As the chemical potential is uniform throughout the system, any change in the local environment directly influences the local densities of all species as predicted by the Euler-Lagrange equation:

$$k_B T \ln \rho_i^b + \mu_i^{ex,b} = k_B T \ln \rho_i(z) + \mu_i^{ex,\text{int}}(z) + \psi(z) Z_i e + V_i^{ext}(z). \tag{15}$$

The left side of Eq. (15) corresponds to the chemical potential of species i in the bulk, whereas the right side is that at position z in the inhomogeneous fluid (i.e., near the interface). Similar to that in the bulk solution, the excess chemical potential $\mu_i^{ex,int}$ accounts for intermolecular interactions

other than the direct Coulomb contribution. The latter is related to the mean electrostatic potential, ψ, which includes contributions from Coulomb interactions between all ionic species and the surface. The last term on the right side of Eq. (15), V_i^{ext}, denotes the non-electrostatic interactions with the surface, i.e., the hard-wall and short-range attraction as given by Eq. (1). It is worth noting that the chemical equilibrium between the different electrostatic states of the amino acid near the surface is naturally satisfied within our cDFT calculations.

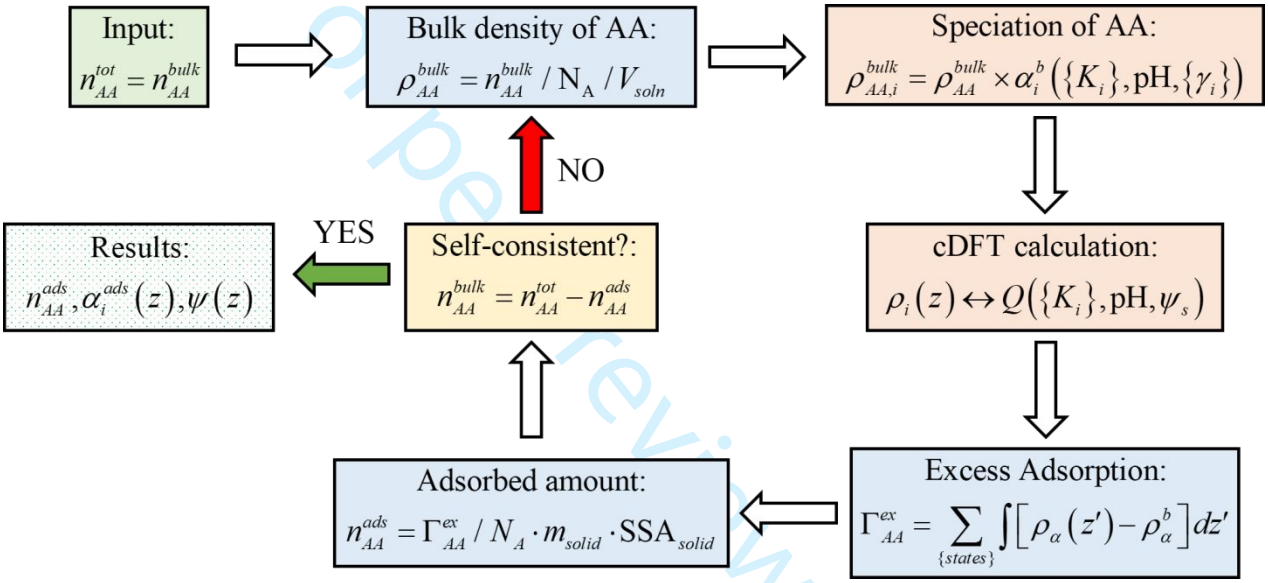

Figure 2. A flowchart of the computational procedure to determine the adsorption of amino acids on an inorganic surface. In consistent with experimental measurements of adsorption isotherms, each cDFT calculation is carried out at a fixed temperature, volume, and the total moles of amino acid n_{AA}^{tot} in the system.

To facilitate direct comparison of the theoretical results with experimental data, we must perform the cDFT calculations for the adsorption of amino acids at an inorganic surface at a fixed total number of amino-acid molecules in the solution. Figure 2 presents a flowchart of our calculation procedure. The total amount of amino acid in the solution includes contributions from both the adsorbed amount on the surface as well as that in the bulk solution, i.e., $n_{AA}^{tot} = n_{AA}^{bulk} + n_{AA}^{ads}$.

However, the cDFT calculation must be performed at a fixed bulk chemical potential, i.e., the bulk density of each species must be known *a priori*. To convert the moles of amino acid in the solution to a bulk density, we must know the solution volume (V_{soln}). We can then relate the total number of moles of the amino acid to its corresponding bulk density by $\rho_{AA}^{bulk} = n_{AA}^{bulk} / N_A / V_{soln}$, where N_{A} is Avogadro's number. Because we explicitly consider the chemical equilibrium between the different ionization states of each amino acid, we must also determine the bulk density for the amino acid at each ionization state. The degree of dissociation at state i is defined by $\alpha_i = \rho_{A_i} / \sum_j \rho_{A_j}$, where the summation extend over all possible charged states of the amino acid. By coupling the degree of ionization with the expressions for protonation/deprotonation equilibrium, we can determine the relative presence of each charged state for the amino acid from

$$\alpha_i = \frac{a_{H^+}^i \prod_{j=1}^{i} K'_j}{1 + \sum_{j=\{states\}} a_{H^+}^j \prod_{k=1}^{j} K'_k} \tag{16}$$

where $K'_j = K_j^T \gamma_{A_{j-1}} / \gamma_j$ is the apparent equilibrium constant defined by the thermodynamic equilibrium constant and the ratio of the bulk activity coefficients.

Eq. (16) can be solved numerically by using known equilibrium constants for different functional groups of the amino acid and the augumented primitive model (APM) to account for thermodynamic non-ideality. Once the bulk density of the amino acid at each charged state has been determined from $\rho_{AA_i}^{bulk} = \rho_{AA}^{bulk} \alpha_i$, cDFT calculation is then performed to determine the adsorption of the amino acid at the inorganic surface. The chemical equilibrium for the protonation/deprotonation of amino acids in the inhomogeneous environment will be automatically satisfied as shown by Eq. (15). During the cDFT calculations, we determine the

density profiles of the amino-acid molecules in different charged states along with the distributions of salt ions. The charge density of the inorganic surface can be calculated from the condition of charge neutrality as shown in Eq. (9). The surface excess for each amino acid, i.e., the amount adsorbed at the surface, is given by

$$\Gamma_{AA}^{ex} = \sum_{\{states\}} \int \left[\rho_\alpha (z') - \rho_\alpha^b \right] dz' . \tag{17}$$

Given the total mass (m_{solid}) and the specific surface area (SSA) of the solid, the excess adsorption can be related to the total adsorbed amount by

$$n_{AA}^{ads} = \Gamma_{AA}^{ex} / N_A \cdot m_{solid} \cdot \text{SSA}_{solid} . \tag{18}$$

As mentioned above, experimental measurements of adsorption isotherms are often reported in terms of the total moles of amino acid in the solution. The sum of amino acids in the bulk and that at the surface must be equal to the total moles in the solution. In our cDFT calculations, we iterate the cDFT calculations with the mole amount in the bulk given by $n_{AA}^{bulk} = n_{AA}^{tot} - n_{AA}^{ads}$ and solve for n_{AA}^{ads} from Eq. (18) until the quantity is converged. After convergence, we can make direct comparison of the theoretical results with experimental data for the adsorbed amount of each amino acid given that the total amino acid in the solution is fixed.

3. Results and Discussion

In the following, we provide 3 case studies to illustrate the application of our coarse-grained model to describe the effects of solution conditions on the adsorption of amino acids on different inorganic surfaces. We first consider the charge regulation of rutile in different salt solutions. Rutile can be either positively or negatively charged depending upon the solution pH. Next, we investigate the adsorption isotherms on rutile (110) surface for the three charge classes of natural amino acids: acidic, basic, and neutral. We find that the adsorption of these amino acids

is highly dependent upon pH, amino acid concentration, and salt concentration in the bulk solution. Due to the protonation/deprotonation of both the amino acid molecules and the rutile surface, the adsorption isotherm typically shows a maximum at an intermediate pH value that is dependent upon the salt type and concentration. In all cases, we find that our coarse-grained model performs well in capturing the adsorption behavior of natural amino acids in different solution conditions.

3.1 *Surface charge of rutile in aqueous NaCl and $CaCl_2$ solutions*

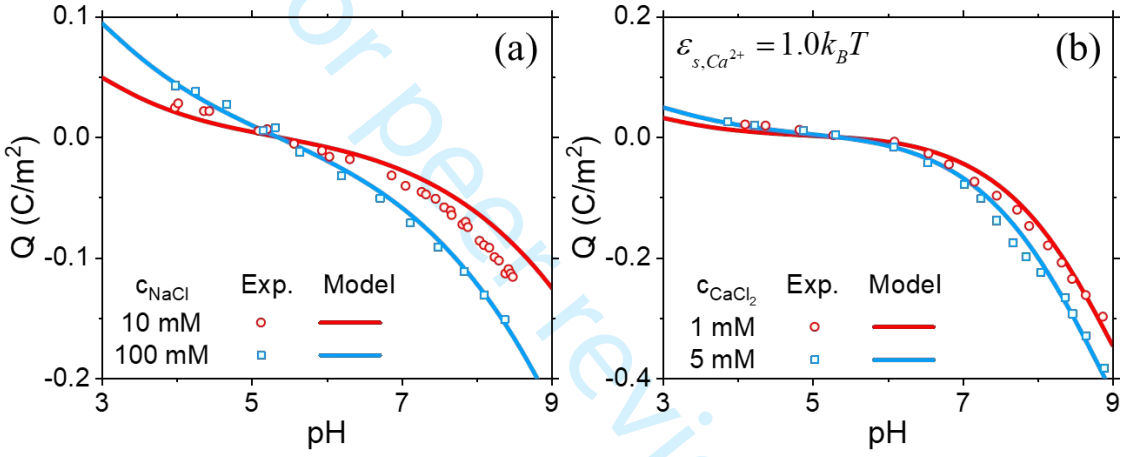

Figure 3. The surface charge density of rutile as a function of pH in (a) NaCl solution and (b) $CaCl_2$ solution from experiment[19,34] (symbols) and from the prediction of the coarse-grained model (lines). The surface site density is fixed at 3 nm^{-2} in agreement with Bahri et al.[19]. The deprotonation and protonation constants are pK_D=6.5 and pK_P=-4.1, respectively.

Charge regulation is important for understanding the adsorption of amino acids at rutile (and other inorganic) surfaces as the adsorption is highly sensitive to electrostatic interactions. Figure 3 shows the surface charge density of rutile in sodium chloride and calcium chloride aqueous solutions at two representative salt concentrations. By employing the augmented primitive model (APM) for aqueous electrolytes, we can describe the surface charge at different pH and salt concentrations by using only the thermodynamic equilibrium constants for protonation

and deprotonation. These two constants are inherently coupled with the isoelectric point of the surface which can be related by $pI = (pK_D - pK_P)/2$. We set the isoelectric point to pI=5.3 consistent with previous experimental findings[35]. Based on this, the deprotonation and protonation constants were determined to be pK_D = 6.5 and pK_P = -4.1, respectively. The surface charge is highly dependent on pH and, to a lesser extent, on sodium chloride concentration. The addition of salt ions to the solution reduces the electrostatic repulsion between surface sites leading to an increase in the surface charge at a fixed pH[17]. APM slightly overestimates electrostatic repulsion between the surface sites as shown by the underestimation of the surface charge at 10 mM. A more sophisticated approach to describe the surface reactions (e.g., multi-site or ion-complexation) could lead to more accurate prediction of the surface charge regulation. As can be seen from Figure 3, the rutile surface is positively charged at low pH (i.e., below its isoelectric point) and negatively charged at high pH. The regulation of the surface charge provides a convenient way to promote or inhibit the adsorption of amino acids or charged organic molecules. We see that APM provides a quantitative description of the effects of the monovalent electrolyte on the surface charge of rutile. A good agreement of the theoretical prediction and experiment was also found for other inorganic surfaces[22,24].

We next consider the surface charge of rutile in calcium chloride solutions. As shown in Figure 3b, the deprotonation of the rutile surface (i.e., increases in negative charge) is less dependent on pH in the presence of calcium ions. The trend is noticeable despite the fact that the concentration of calcium ions is one order of magnitude smaller than that of sodium ions (e.g., 1 mM $CaCl_2$ vs. 10 mM NaCl). Such behavior can be attributed to the stronger electrostatic binding between the negatively charged surface sites and the divalent cation. On the other hand, when rutile is positively charged, the influence of the cation valence is negligible as it is the monovalent

chloride ions dictating the surface charge density. To match the experimental data for rutile in the presence of calcium chloride, we used the same equilibrium constants determined for rutile in sodium chloride solutions. However, this led to a consistent underestimation of the surface charge above the isoelectric point. Previous studies have demonstrated the importance of calcium binding to surface hydroxyl sites beyond electrostatic attraction[36]. It has also been suggested that the hydration of the calcium ion near the surface is different from that in the bulk[37]. To account for such effects, we introduced a short-range attraction of magnitude ε_{surf} = 1.0 k_BT between the calcium ions and the rutile surface to mimic this non-electrostatic binding behavior. The inclusion of this short-range attraction leads to a perfect description of the ionization behavior of rutile in the presence of calcium chloride.

3.2 *Adsorption of acidic amino acids to rutile*

The adsorption of amino acids at inorganic surfaces is complicated by the fact that both the amino acid and surface are ionizable and that the surface forces are highly sensitive to the solution pH and local ion concentrations. Due to competing electrostatic interactions, the adsorption isotherm is often nonmonotonic with respect to pH and shows a strong dependence on solution conditions (e.g., salt type and concentration). To elucidate, Figure 4 presents the adsorption of glutamic acid and aspartic acid at a rutile surface versus pH at several sodium chloride and amino acid concentrations. The adsorption of both acidic amino acids shows a maximum near the pK_a value of the amino-acid side chain. At this condition, approximately 50% of the acidic amino acids carry a negative charge. A reduction of the pH below the pK_a would shift the equilibrium to the neutral state while an increase in pH would result in the amino acids existing predominately in their negatively charged state. Meanwhile, the rutile surface exhibits a positive charge below its isoelectric point of pI=5.3, which leads to a pH window where the adsorption is favored by the

electrostatic interaction between the surface and the amino acid. Surprisingly, significant adsorption is observed even at pH=9 where there is a strong electrostatic repulsion between the acidic amino acids and the negatively charged surface. In this case, the adsorption can be attributed to hydrogen bonding between the carboxyl groups from the amino acids and the surface hydroxyl sites[38,39]. Such interaction can be modeled through a square-well potential between the amino acid and the surface, irrespective of the charge status. We determined the fitting parameter to be ε_{surf} =9.6 k_BT based off a comparison with the experimental adsorption data for 0.5 mM amino acid and 100 mM sodium chloride solution. Due to similarities in the chemical structure of both acidic amino acids, it is expected that the two will interact similarly with the rutile surface. Therefore, we did not distinguish the surface binding energy between the two amino acids which, as demonstrated by Figure 4, was found to be satisfactory.

As expected, the solution condition has an important effect on the adsorption of acidic amino acids at the rutile surface. In general, the adsorbed amount increases with the total concentration of amino acid in the solution. For example, the mean lateral separation between glutamic acid on the rutile surface at pH 3 decreases from approximately 3 nm (~0.2 μmol/m^2) to 1 nm (~1.5 μmol/m^2) when the concentration of glutamic acid is increased from 0.1 mM to 2.0 mM. Such effect is most noticeable at low pH because the opposite surface charge leads to a stronger driving force for the adsorption. While the amino-acid concentration has little effect on the solution pH at which the maximum in adsorption occurs, the salt concentration results in a notable shift in the pH at which the adsorption is maximized. The variation of the salt concentration will also influence the adsorption of charged amino acids because of the electrostatic screening effect.

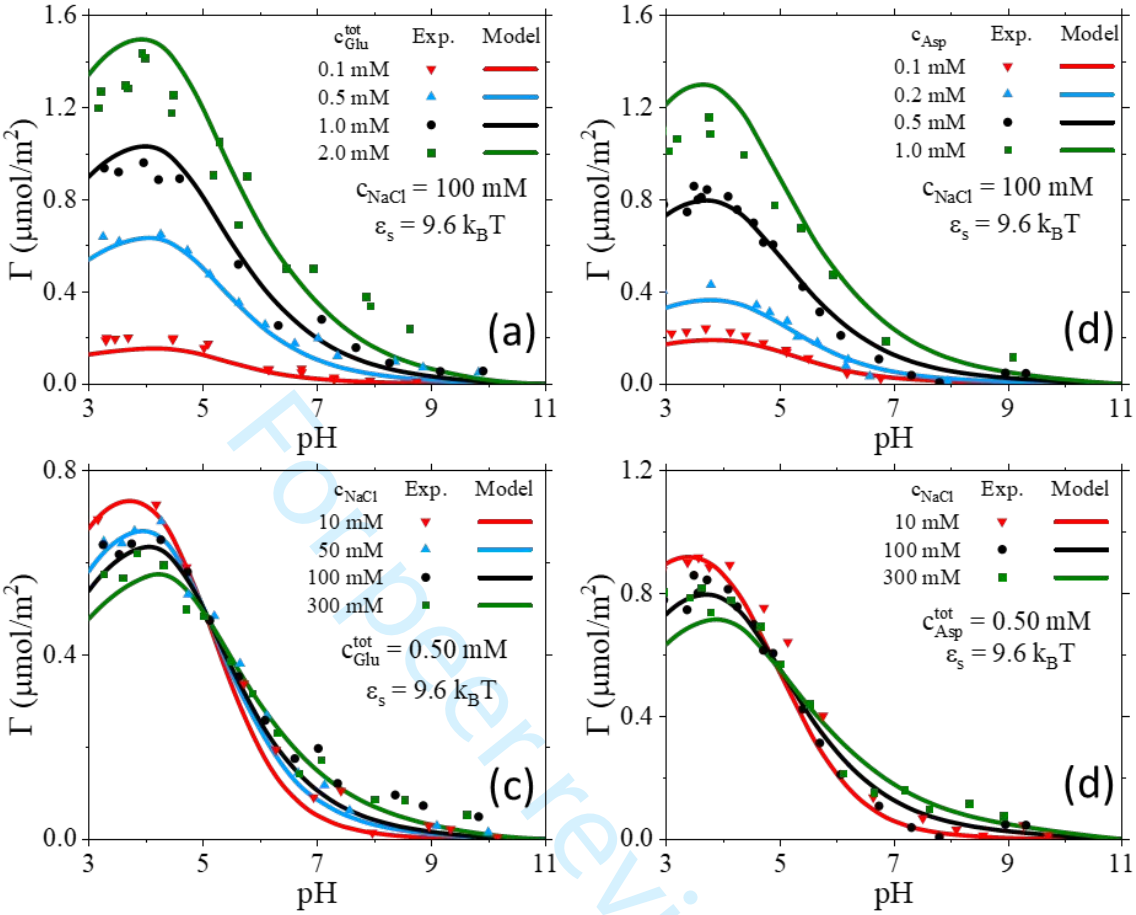

Figure 4. The pH-dependent adsorption of glutamic acid and aspartic acid on the rutile surface at (a and b) various total concentrations of amino acids in a 100 mM aqueous NaCl solution and (c and d) several NaCl concentrations in a 0.50 mM aqueous amino acid solution. The symbols are from experiment[19], and the lines are predictions of the coarse-grained model.

It has been well documented that the addition of salt ions to the solution will promote ionization of the inorganic surface by decreasing the electrostatic repulsion between the surface sites (as shown previously in Figure 3). However, it is not clear how the distribution of charged states for the amino acid is affected by the increase in salt concentration. While the ionized forms of the amino acid would be typically favored by increasing the salt concentration in the bulk solution, the reduced Coulomb interaction with the surface sites may be more impactful on amino-acid speciation. Since an increase in the salt concentration shifts the maximum adsorption to a

higher pH (i.e., the chemical equilibrium shifts to the negatively charged state of the amino acid), we expect that, at a fixed pH, the addition of salt inhibits amino acids in the ionized state. This is because a weaker interaction with the positively charged surface by the negatively charged amino acid reduces the preference of the amino acid in its anionic state.

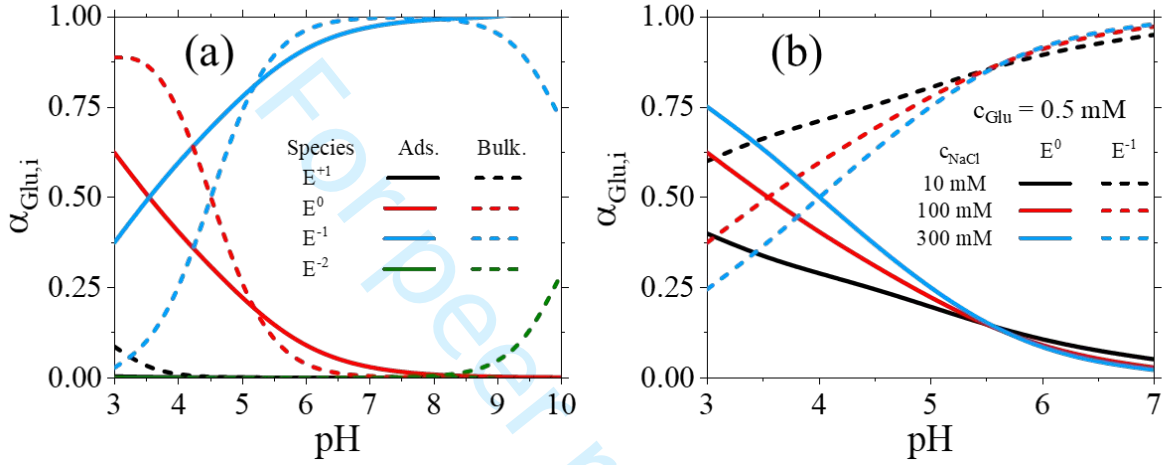

Figure 5. (a) The pH-dependent speciation of glutamic acid at the rutile surface and in the bulk solution. The total concentration of glutamic acid is 0.5 mM, and the NaCl concentration is 100 mM. (b) Speciation of adsorbed glutamic acid into its two predominant states, neutral and negatively charged, in the pH range of 3 to 7 at three NaCl concentrations (10, 100, and 300 mM).

The interfacial behavior of amino acids at inorganic surfaces are dependent on their ionization states near the surface. In most cases, the dominate charge state at the surface is significantly different from that in the bulk solution due to the selective interactions of the surface with amino acid molecules. To demonstrate this, we show in Figure 5a the pH-dependent speciation of glutamic acid in the bulk solution and on the rutile surface in 100 mM sodium chloride solution. At low pH, the amino acid is dominated by its negatively charged state due to strong Coulomb interactions with the positively charged surface sites on rutile while the amino acid mostly exists in its neutral state in the bulk solution (i.e., far from the surface). There is a

small reversal in this trend as the pH is increased because the rutile surface transitions to negatively charged and repulses the anionic state of the amino acid. At higher pH, the monovalent anionic state is maintained somewhat more than that in the bulk solution to avoid the repulsion between the negatively charged surface and amino-acid molecules in the divalent anionic state. Based off these results, it also becomes clear why there is a maximum in the adsorption at low pH seen in Figure 4. While the surface has more positive charge as pH falls, it adsorbs less amino acid even though it is negatively charged. This interplay between a stronger electrostatic attraction but a lower concentration of amino acids in the anionic state leads to the maximum adsorption in responding to the pH changes. Although the positively charged surface promotes the ionization of the acidic amino acid relative to the bulk solution, the increased electrostatic force is insufficient to compensate the reduction in the concentration of a negatively charged amino acid.

Figure 5b shows the influence of salt concentration on the speciation of the adsorbed amino acid molecules in neutral and negatively charged states. It is clear that the salt concentration plays a key role on speciation at low pH where the adsorption is mostly driven by electrostatic forces. At low pH, an increase in the salt concentration disfavors the presence of the amino acid in the negatively charged state. Interestingly, an opposite trend is observed as the salt concentration in the bulk solution rises[40]. In the former case, the addition of salt weakens the electrostatic attraction between the rutile surface and amino acid molecules (*viz*. through the reduction of the mean electrostatic potential). The electrostatic interaction is responsible for the increased population of the anionic state near the surface while the bulk solution is dominated by amino-acid molecules in the neutral state. The increase in the salt concentration reduces the mean electrostatic potential at the surface leading to a reduction of the local concentration of the amino acid in the negatively charged state. At these conditions (e.g., low pH and small salt concentration), the ionic excluded-

volume effects and electrostatic correlations are relatively insignificant in the ionization behavior of the acidic amino acid. Therefore, an accurate description of charge regulation for both the amino acid and the surface is essential for understanding the adsorption of amino acids at the rutile surface.

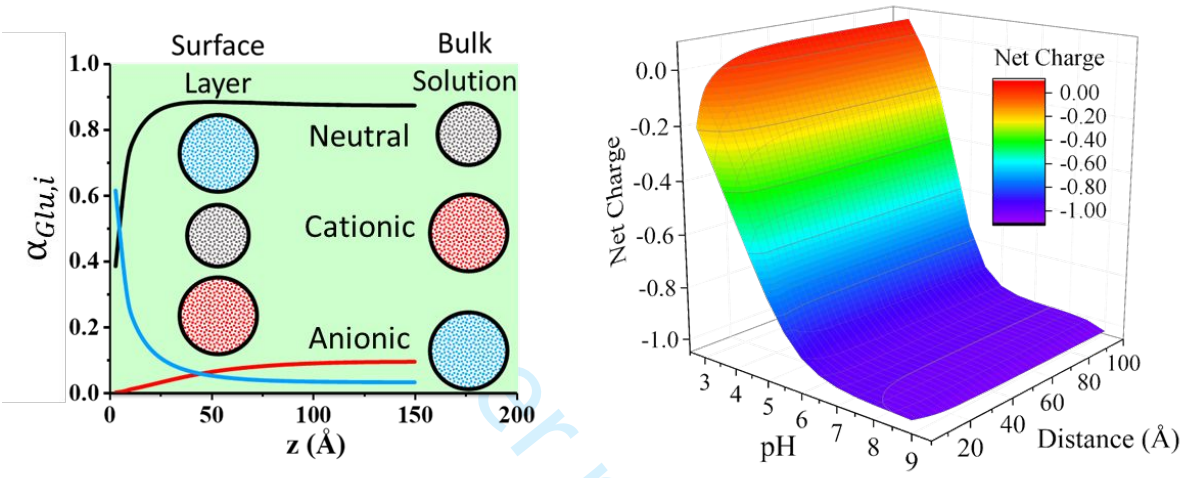

Figure 6. (a) The speciation of glutamic acid as a function of the distance from the surface at pH=3. (b) The net charge of the glutamic acid as a function of the distance from the surface and pH. In both cases, the total concentration of glutamic acid is 0.5 mM, and the NaCl concentration is 100 mM.

The presence of rutile, particularly when it is highly charged, leads to a significantly different speciation of the amino acid near the surface from that in the bulk solution. The variation in local ionization may span up to a few nanometers depending on the salt concentration. In Figure 6a, we present theoretical predictions for the speciation of glutamic acid as a function of the distance from the surface at pH=3.0. In this case, the rutile surface is positively charged as previously shown in Figure 3. The strong electrostatic attraction between the amino acid in the negatively charged state and the positively charged surface shifts the protonation equilibrium of the amino acid to the anionic state. Meanwhile, the amino acid in neutral and cationic states, which

dominate in the bulk solution, are depleted near the surface. While amino acids typically show monolayer adsorption and thus the long-range ionization behavior is of less significance, the strong variation in speciation near the surface results in drastic differences between the composition of the adsorbed layer and that in the bulk solution. On the other hand, the long-range ionization behavior may find more importance in the adsorption of polypeptides and proteins due to strong intrachain correlations.

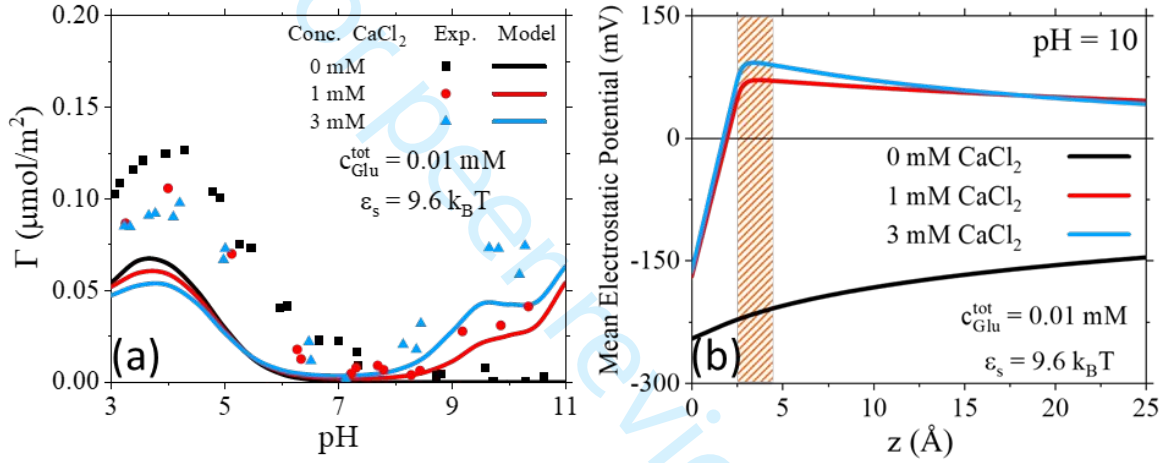

Figure 7. (a) The pH-dependent adsorption of glutamic acid on the rutile surface at different concentrations of $CaCl_2$ in 0.01 mM aqueous glutamic acid solution from experiment[36] (symbols) and the theoretical prediction (lines). (b) The mean electrostatic potential as a function of the distance from the rutile surface for the adsorption of glutamic acid at pH = 10 from salt-free and 1 or 3 mM $CaCl_2$ solutions. The shaded region corresponds to a monolayer of glutamic acid adsorbed at the surface.

We show in Figure 6b how the net charge of glutamic acid varies with the distance from the rutile surface and pH. In general, the net charge is shifted towards the charged state that favors interaction with the surface. At low pH, the glutamic acid has a positive net charge in the bulk solution while the rutile surface is also positively charged. In this case, the net charge is reduced

as the amino acid is positioned close to surface. The opposite occurs at high pH with the net charge increasing near the surface since rutile is negatively charged at these conditions. Again, an accurate description of the charge regulation for both the surface and amino acid is important to predict how changes in the environment affect the amino-acid adsorption.

Next, we consider the role of multivalent ions in facilitating the adsorption of amino acids. Because of electrostatic correlations, significant adsorption may take place in the presence of multivalent ions despite that the amino acid and the surface have the same sign of electric charge. Figure 7 shows the adsorption of glutamic acid at the rutile surface in a salt-free solution and two calcium chloride solutions of different concentrations. For both glutamic acid and calcium ions, the surface energy parameters are the same as those determined previously. For the salt-free case, glutamic acid exhibits a maximum adsorption at low pH with little to no adsorption when pH>7. Qualitatively, the pH effect is consistent with the adsorption at higher amino-acid concentrations as previously shown in Figure 4. The addition of calcium ions to the solution leads to significant adsorption of the glutamic acid at high pH when both the amino acid and the rutile surface are negatively charged.

To understand the origin of attraction, we show in Figure 7b the mean electrostatic potential as a function of the distance at pH=10 for the three aqueous solutions considered in Figure 7a. For the salt-free case (i.e., 0 mM $CaCl_2$), the mean electrostatic potential is strongly negative at the surface and decays slowly with the distance as predicted by a conventional electric double layer (EDL) model. However, in the presence of calcium ions, the surface potential is significantly reduced and the local electrostatic potential switches in sign (i.e., from negative to positive) signaling charge inversion. In other words, the surface charge is overcompensated by the oppositely charged ions through specific association and electrostatic correlations[41]. The charge

inversion leads to the adsorption of the negatively charged glutamic acid which experiences an effective attraction to the overcompensated "positive" surface despite itself being negatively charged. Although the agreement between experiment and theoretical predictions is only semi-quantitative, Figure 7 clearly demonstrates that our model captures the important physics regarding the effect of multivalent ions on the adsorption of amino acids at inorganic surfaces.

3.2 *Adsorption of basic amino acids*

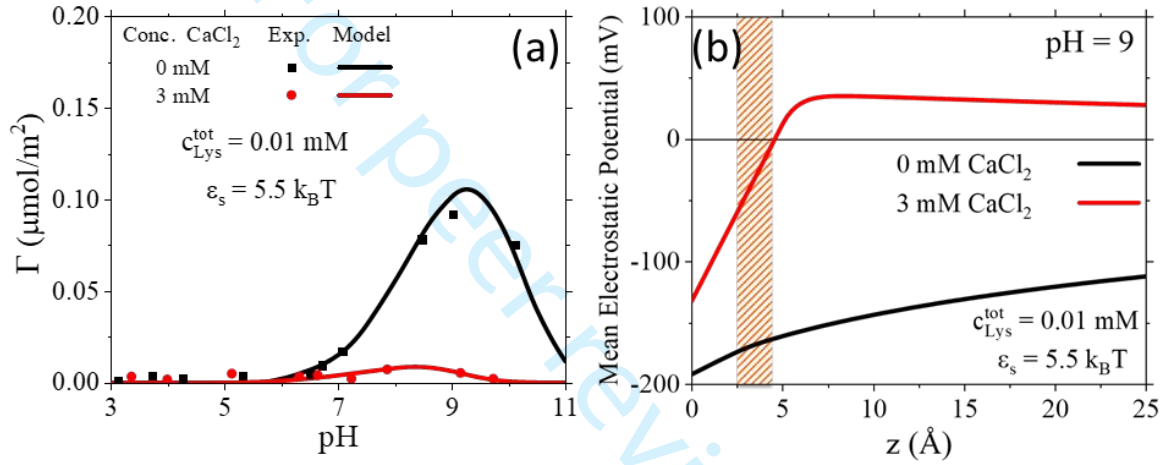

Figure 8. (a) The pH-dependent lysine adsorption at the rutile surface from experiment[36] (symbols) and the theoretical prediction (lines). (b) The mean electrostatic potential as a function of the distance from the rutile surface in two aqueous solutions at pH=9. Approximately, the shaded area corresponds to a monolayer of lysine at the rutile surface.

We now turn our attention to the adsorption of lysine, a basic amino acid, at the rutile surface. In the bulk solution, lysine molecules mostly exist in its positively charged state, except for high pH (i.e., pH>9) where its backbone amine group will deprotonate shifting the equilibrium to its neutral state. Further increase in the pH will result in the side-chain amine group also deprotonating and the anionic state of lysine becoming dominant. Figure 8 shows the adsorption of lysine at the rutile surface in a salt-free solution and that in a 3 mM calcium chloride solution.

While aspartic acid and glutamic acid display significant adsorption when they have the same electric charge as the surface, lysine shows no adsorption at similar conditions. Interestingly, no significant adsorption is observed even when the surface is neutral or weakly charged with a negative sign. The non-adsorption behavior can be attributed to the limited binding capability of its side chain with the rutile surface. In contrast to the carboxyl group in the side chain of aspartic or glutamic acid, there is less significant binding between the amine group in the lysine side chain with the hydroxyl groups from the rutile surface. In our coarse-grained model, the non-electrostatic effect is captured by a lower binding energy of each lysine molecule with the surface, ε_{surf} =5.5 k_BT, compared with 9.6 k_BT for the acidic amino acids. As a result, the electrostatic interactions play a more dominant role in lysine adsorption at the rutile surface.

When the solution pH is above the isoelectric point of the rutile surface (pI = 5.3), lysine molecules and the surface have opposite charges and the electrostatic attraction leads to strong adsorption of the amino acid. However, the adsorption shows a maximum at pH=9 beyond which it falls as a result of the increased prevalence of lysine molecules in the neutral state. The situation is similar to that found for acidic amino acids at low pH. In the presence of calcium ions, the adsorption of lysine drops dramatically compared to the salt-free case. This is not surprising because the divalent cations outcompete the monovalent lysine. As the non-electrostatic binding energy is relatively insignificant in comparison with that for acidic amino acids, lysine adsorption is more sensitive to the screening effects due to salt ions in the solution.

Figure 8b shows how the local electrostatic potential varies with the distance from the rutile surface. As discussed above, the presence of calcium ions leads to a significant reduction of the surface electric potential. The charge inversion hinders the adsorption of lysine molecules at the rutile surface even though the amino acid and the surface have opposite charges. The competition

in adsorption between the amino acid and the multivalent ions to the rutile surface is well captured by our coarse-grained model.

3.3 *Adsorption of neutral amino acids*

Lastly, we consider the adsorption of a neutral amino acid, dihydroxyphenylalanine (DOPA), to the rutile surface. From the practical perspective, understanding DOPA adsorption is highly important due to its extensive use in bioadhesive materials[42-44]. DOPA exhibits excellent adhesive and cohesive properties through its strong binding to inorganic surfaces by a bidentate bonding of its two hydroxyl groups in the side chain and complexation with multivalent ions by its aromatic group, respectively[45]. While most neutral amino acids show little or no adsorption at inorganic surfaces[18], DOPA displays strong adsorption that is highly dependent on the solution pH and salt concentration.

As demonstrated by spectroscopy measurements[46], DOPA binds with an inorganic surface in one of two configurations: lying flat or standing up. When a DOPA molecule is in its flat configuration, it interacts with the surface through its carboxyl group in the backbone and the two hydroxyl groups in its side chain. Meanwhile, the standing up orientation allows only for the interaction of the two hydroxyl groups with the surface. Since these configurations are dependent upon the availability of specific surface sites, the solution pH has noticeable effects on both the adsorption and configuration of DOPA due to the protonation or deprotonation of the surface sites.

In order to accurately describe the adsorption of DOPA to an inorganic surface, we must acknowledge the existence of these two orientations at the surface. Barhi et al. employed an extended triple layer model that describes DOPA attachment to the surface through either four or two surface sites[47]. The former corresponds to the lying flat orientation where the two phenolic oxygens and one of the carboxylate oxygens bind to the titanium atom on the surface while the

other carboxylate oxygen is hydrogen bonded to a hydroxyl group at the surface. On the other hand, the complexation with two surface sites involves one of the phenolic oxygens bonding to the titanium atom while the other phenolic oxygen is involved with hydrogen bonding to the surface. The surface complexation scheme can be described through the following chemical reactions[47]:

$$4-\mathrm{TiOH}+\mathrm{H_3DP}\leftrightarrow\left(-\mathrm{TiOH}\right)-\mathrm{Ti_3DP}+3\mathrm{H_2O} \tag{19}$$

$$2-\mathrm{TiOH}+\mathrm{H_3DP}\leftrightarrow\left(-\mathrm{TiOH_2^+}\right)-\mathrm{TiHDP^-}+\mathrm{H_2O} \tag{20}$$

where H_3DP represents DOPA in its neutral state. The thermodynamic equilibrium constants for these reactions can be related to the activities of the pertinent species by

$$K_{(-\mathrm{TiOH})-\mathrm{Ti_3DP}}=\frac{a_{(-\mathrm{TiOH})-\mathrm{Ti_3DP}}a_{\mathrm{H_2O}}^3}{a_{-\mathrm{TiOH}}^4 a_{\mathrm{H_3DP}}}\exp\left[\beta e\Delta\psi_{r,1}\right], \tag{21}$$

$$K_{\left(-\mathrm{TiOH_2^+}\right)-\mathrm{TiHDP^-}}=\frac{a_{\left(-\mathrm{TiOH_2^+}\right)-\mathrm{TiHDP^-}}a_{\mathrm{H_2O}}}{a_{-\mathrm{TiOH}}^2 a_{\mathrm{H_3DP}}}\exp\left[\beta e\Delta\psi_{r,2}\right]. \tag{22}$$

The inclusion of the exponential term results from the electrical work involved with moving ions and/or water dipoles to and from the surface[26]. The electrostatic work to displace water dipoles from the surface is given by $\Delta\psi_{\mathrm{H_2O}}=-n_{\mathrm{H_2O}}(\psi_s-\psi_\beta)$, where $n_{\mathrm{H_2O}}$ represents the stoichiometric coefficient of water molecules on the right-hand side of the reactions in Eqs. (19) and (20), ψ_s and ψ_β refer to the electric potentials at the surface and at the plane at which the DOPA molecule is adsorbed (i.e., when in contact with the surface, $z=\sigma_{DP}/2$). The electrical work involved in the first reaction is

$$\Delta\psi_{r,1}=3\psi_s-3\psi_\beta-3\left(\psi_s-\psi_\beta\right)=0 \tag{23}$$

where the three terms in the middle correspond to changes in the potentials experienced by the three H^+ ions adsorbing to the surface, the DP^{3-} ion adsorbing to the β-plane, and three H_2O

molecules desorbing from the surface, respectively. Thus, there is no contribution by the electrical work involved with moving ions and water molecules to and from the surface. On the other hand, the electrical work of the second reaction is

$$\Delta\psi_{r,2} = 2\psi_s - 2\psi_\beta - \left(\psi_s - \psi_\beta\right) = \psi_s - \psi_\beta \tag{24}$$

where the three terms in the middle correspond to changes in the electric potentials experienced by the two H^+ ions adsorbed at the surface, the HDP^{2-} ion adsorbed at the β-plane, and H_2O molecule desorbed from the surface, respectively. Based off the fitting with the experimental data, we determined the negative logarithmic equilibrium constants for the two reactions to be 11.6 and 5.8, respectively. The pK_a values are slightly different from those determined by Bahri et al. (11.8 and 6.4, respectively). The difference is expected because we consider thermodynamic non-ideality in addition to the direct Coulomb interactions.

We show in Figure 9a and b the adsorption of DOPA to the rutile surface versus the solution pH at different salt and total DOPA concentrations. The adsorption of most neutral amino acids shows little sensitivity to pH since they are not directly influenced by changes in the surface charge[48]. This is valid except at very low or high pH values when the ionized state of the amino acid becomes dominate. For example, a neutral amino acid typically carries a positive charge at pH<2 while the rutile surface is also positively charged. Similar to other neutral amino acids, the DOPA adsorption is reduced when the ionized states are favored at extreme pH values. However, DOPA adsorption varies with pH even though the molecule is entirely in its neutral state. Because of its association with the surface sites (i.e., TiOH), the surface sites in protonated ($TiOH_2^+$) or deprotonated (TiO^-) states will impact DOPA adsorption.

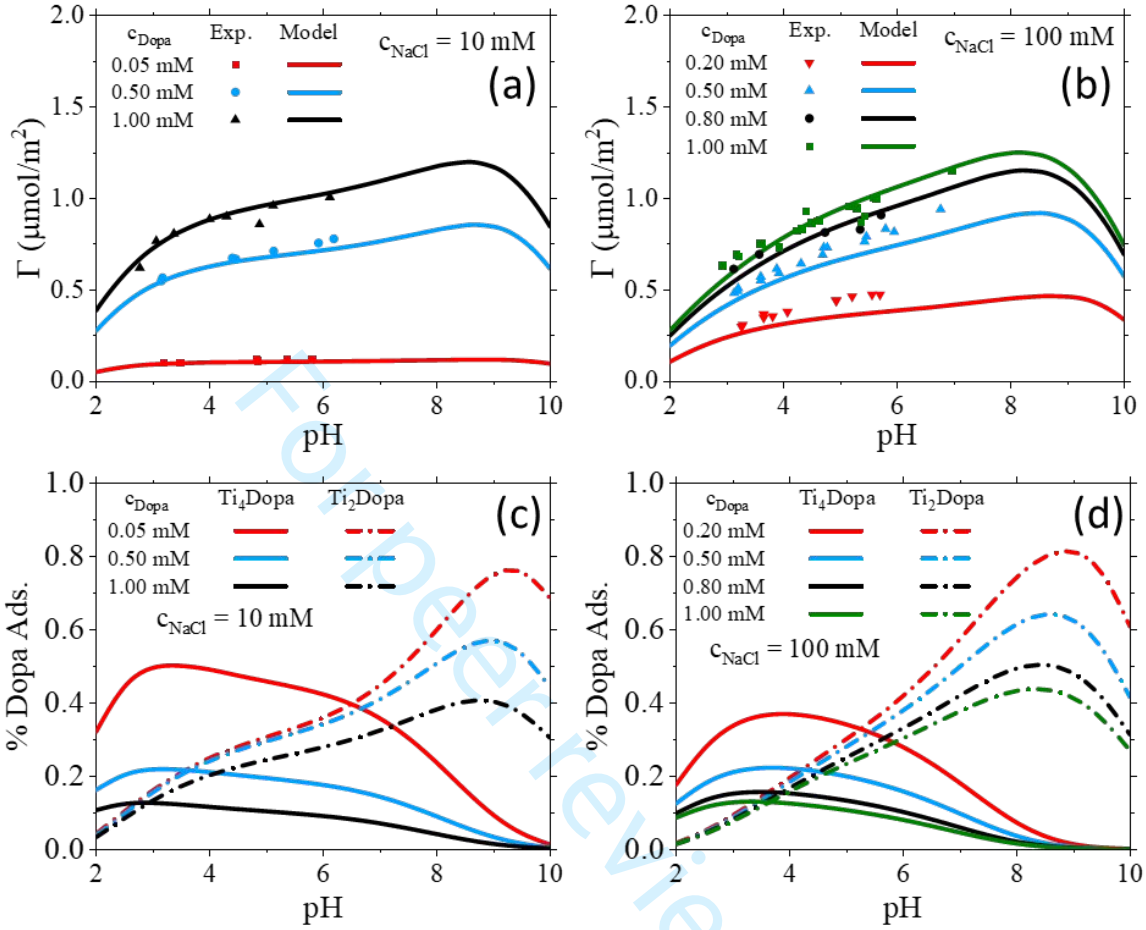

Figure 9. The adsorption of dihydroxyphenylalanine (DOPA) at the rutile surface versus pH in (a) 10 mM and (b) 100 mM NaCl solutions. Different lines are theoretical predictions corresponding to various total DOPA concentrations, the symbols are from experiment[47]. The speciation of DOPA at the rutile surface as a function of pH predicted according to the thermodynamic model. Ti_nDOPA refers to the binding of DOPA to *n* titanium surface sites as given by Eqs. (21) and (22).

To understand further why DOPA adsorption increases as the pH rises, we may consider the distribution of adsorbed DOPA according to the surface configurations:

$$n_{DP}^{ads} = n_{(>\mathrm{TiOH})>\mathrm{Ti_3DP}} + n_{(>\mathrm{TiOH_2^+})>\mathrm{TiHDP^-}}. \quad (25)$$

Based off the conditions of chemical equilibrium as shown in Eqs. (21) and (22), we may relate the surface concentrations of DOPA in different configurations to the number density of surface hydroxyl groups:

$$n_{DP}^{ads} = \mathrm{K}_1' n_{\mathrm{TiOH}}^4 c_{\mathrm{DP}} + \mathrm{K}_2' \exp\left[-\beta e \Delta\psi_{r,2}\right] n_{\mathrm{TiOH}}^2 c_{DP} \tag{26}$$

where indices 1 and 2 refer to the chemical reactions involving four and two surface sites, respectively, and the primes denote the apparent equilibrium constants, i.e., after the conversions from activity to the number density or concentration. Eq. (26) indicates that DOPA adsorption is intrinsically related to the availability of surface hydroxyl sites and the DOPA concentration at the surface. As the number density of surface hydroxyl sites decreases as the pH deviates from the isoelectric point, we expect that the DOPA adsorption will be maximized near the isoelectric point. Meanwhile, the exponential factor in the second term on the right side of Eq. (26) explains why DOPA adsorption increases with pH beyond the isoelectric point. When the surface is positively charged, $\Delta\psi_{r,2}$ is greater than zero; and it is less than zero when the surface is negatively charged, i.e., the surface potential is always greater in magnitude than that at the adsorption plane of DOPA. Because the magnitude of $\Delta\psi_{r,2}$ increases as the pH deviates more from the isoelectric point, the exponential term approaches unity from below as the pH increases towards the isoelectric point. Further increase in the pH will increase the absolute value of the exponential factor and thus improve the adsorption of DOPA. Therefore, we conclude that the increase in DOPA adsorption with pH results from the favorable electrostatic work due to the complexation of the DOPA molecule with the surface. The importance of electrostatic interactions in the binding of a neutral DOPA molecule with the rutile surface explains why the salt concentration plays a significant role in the adsorption.

Figure 9c and d present the fraction of DOPA in two surface configurations. The electrostatic work is a contributing factor for DOPA transition from lying flat to standing up as the pH rises. The increase in salt concentration tends to shift the transition between the two surface configurations to a lower pH due to electrostatic screening. Another major factor in determining the surface configuration of DOPA is its local number density. When the surface concentration of DOPA increases, it lowers the pH at which the transition takes place due to the competition of DOPA molecules with each other at the surface. At small surface concentrations, the competition for the surface sites is less important, which explains why the DOPA molecules are mostly lying flat at the surface. Clearly, the surface complexation model provides a satisfactory description of DOPA adsorption to the titanium surface and valuable insight into the mechanisms of DOPA attachment to inorganic surfaces in an aqueous solution.

4. Conclusion

There have been substantial interests in understanding the interaction of polypeptides and proteins with inorganic surfaces due to their applications to the design of bioadhesives and the remediation of biofouling. In the present study, we have initiated a theoretical work for such possibilities by employing a coarse-grained model for amino acids that captures their adsorption at an inorganic surface under different solution conditions. By leveraging our previous work to account for the key physics governing charge regulation and the interaction of amino acids with ionic species in aqueous solutions, we developed a molecular-thermodynamic framework that is able to predict the adsorption of amino acids on inorganic surfaces driven by either electrostatic binding or surface complexation. The thermodynamic model integrates ionization equilibrium for both amino acids and inorganic surfaces with the classical density functional theory (cDFT) that facilitates an accurate description of the inhomogeneous distributions of amino acids and ionic

species near inorganic surfaces. Importantly, this model accounts for both chemical and physical interactions between amino acids and an inorganic surface, which is key to capturing the changes in adsorption due to variation in solution conditions.

To demonstrate the effectiveness of this molecular thermodynamic model, we compare theoretical predictions directly with experimental adsorption data for different charge types (i.e., acidic, basic, and neutral) of amino acids on a rutile surface. We first showed that the deprotonation and protonation of hydroxyl sites at the inorganic surface can be well described by coupling the chemical equilibrium of the surface sites with cDFT calculation for ion distributions. We then investigated the adsorption behavior of different amino acids at the rutile surface in aqueous solutions that are varied in pH, amino acid concentration, salt type and concentration. We found that amino-acid adsorption typically shows a maximum an intermediate pH value that is dependent upon the salt type and concentration. While the increase in salt concentration promotes the ionization of the surface sites, it also weakens the electrostatic interaction between amino acid and the surface. Therefore, the addition of salt reduces the adsorption of amino acid and shifts the pH to a higher value where the maximum adsorption takes place. For acidic amino acids, the non-electrostatic surface binding makes a significant contribution to the adsorption even when the electrostatic charges of the amino acid and the surface are of the same sign. On the other hand, a basic amino acid like lysine shows much weaker dependence on non-electrostatic surface binding and the adsorption is mostly driven by electrostatic attraction from the surface. A maximum adsorption takes place at high pH when the amino acid and surface are oppositely charged. Lastly, we considered the adsorption of DOPA, a neutral amino acid, to the rutile surface through a combination with the surface complexation model that accounts for the two configurations of DOPA molecules at the rutile surface.

An accurate description of the charge regulation for both amino acids and the underlying surface in a highly inhomogeneous environment plays an important role in understanding the adsorption behavior of amino acids, particularly the acidic and basic amino acids, to inorganic surfaces. The interaction between amino acids and the surface also affects equilibrium between different charged states leading to the speciation amino acid molecules significantly different from that in the bulk solution. Because of the shift in speciation, the amino acids adsorbed at a highly charged surface may exist in an ionized state of opposite charge of the surface while those in the bulk solution are entirely neutral. Although the molecular-thermodynamic model employs a number of semi-empirical parameters, it provides a predictive description of thermodynamic non-idealities that are relevant to describe the environmental effects on both amino-acid adsorption and chemical equilibrium. In the future, we plan to extend this molecular-thermodynamic framework to describing the adsorption of polypeptides and flexible proteins which are of keen interest for practical applications.

Acknowledgements

This work is supported by the National Science Foundation Harnessing the Data Revolution Big Idea under Grant No. NSF 1940118. Additional support is provided by the National Science Foundation Graduate Research Fellowship under Grant No. DGE-1326120. The computational work used resources of the National Energy Research Scientific Computing Center (NERSC), a DOE Office of Science User Facility supported by the Office of Science of the U.S. Department of Energy, under Contract DE-AC02-05CH11231.

Data Sharing and Data Availability: The data that support the findings of this study are available from the corresponding author upon reasonable request.

References:

1. Balkenende DWR, Winkler SM, Messersmith PB. Marine-inspired polymers in medical adhesion. *European Polymer Journal.* 2019;116:134-143.
2. Adamczyk Z. Protein adsorption: A quest for a universal mechanism. *Current Opinion in Colloid & Interface Science.* 2019;41:50-65.
3. Mahmoudi M. Debugging Nano–Bio Interfaces: Systematic Strategies to Accelerate Clinical Translation of Nanotechnologies. *Trends in Biotechnology.* 2018;36(8):755-769.
4. Schwaminger S, Blank-Shim SA, Borkowska-Panek M, et al. Experimental characterization and simulation of amino acid and peptide interactions with inorganic materials. *Eng Life Sci.* 2018;18(2):84-100.
5. Costa D, Savio L, Pradier CM. Adsorption of Amino Acids and Peptides on Metal and Oxide Surfaces in Water Environment: A Synthetic and Prospective Review. *The Journal of Physical Chemistry B.* 2016;120(29):7039-7052.
6. Kitadai N, Yokoyama T, Nakashima S. ATR-IR spectroscopic study of L-lysine adsorption on amorphous silica. *Journal of Colloid and Interface Science.* 2009;329(1):31-37.
7. Lambert JF. Adsorption and polymerization of amino acids on mineral surfaces: a review. *Orig Life Evol Biosph.* 2008;38(3):211-242.
8. Shchelokov A, Palko N, Potemkin V, et al. Adsorption of Native Amino Acids on Nanocrystalline TiO2: Physical Chemistry, QSPR, and Theoretical Modeling. *Langmuir.* 2019;35(2):538-550.
9. Greiner E, Kumar K, Sumit M, et al. Adsorption of l-glutamic acid and l-aspartic acid to γ-Al2O3. *Geochimica et Cosmochimica Acta.* 2014;133:142-155.
10. Begonja S, Rodenas LAG, Borghi EB, Morando PJ. Adsorption of cysteine on TiO2 at different pH values: Surface complexes characterization by FTIR-ATR and Langmuir isotherms analysis. *Colloids and Surfaces A: Physicochemical and Engineering Aspects.* 2012;403:114-120.
11. El Shafei GMS, Moussa NA. Adsorption of Some Essential Amino Acids on Hydroxyapatite. *Journal of Colloid and Interface Science.* 2001;238(1):160-166.
12. Imamura K, Mimura T, Okamoto M, Sakiyama T, Nakanishi K. Adsorption Behavior of Amino Acids on a Stainless Steel Surface. *Journal of Colloid and Interface Science.* 2000;229(1):237-246.
13. O'Connor AJ, Hokura A, Kisler JM, Shimazu S, Stevens GW, Komatsu Y. Amino acid adsorption onto mesoporous silica molecular sieves. *Separation and Purification Technology.* 2006;48(2):197-201.
14. Horányi G. Adsorption of primary amino compounds at platinum electrodes: A survey of radiotracer studies. *Electrochimica Acta.* 1990;35(6):919-928.
15. Hughes ZE, Walsh TR. What makes a good graphene-binding peptide? Adsorption of amino acids and peptides at aqueous graphene interfaces. *Journal of Materials Chemistry B.* 2015;3(16):3211-3221.
16. Dasetty S, Barrows JK, Sarupria S. Adsorption of amino acids on graphene: assessment of current force fields. *Soft Matter.* 2019;15(11):2359-2372.
17. Hoefling M, Iori F, Corni S, Gottschalk KE. Interaction of amino acids with the Au(111) surface: adsorption free energies from molecular dynamics simulations. *Langmuir.* 2010;26(11):8347-8351.

18. Vlasova N, Golovkova L. The adsorption of amino acids on the surface of highly dispersed silica. *Colloid J+.* 2004;66(6):657-662.
19. Jonsson CM, Jonsson CL, Sverjensky DA, Cleaves HJ, Hazen RM. Attachment of l-Glutamate to Rutile (α-TiO2): A Potentiometric, Adsorption, and Surface Complexation Study. *Langmuir.* 2009;25(20):12127-12135.
20. Jonsson CM, Jonsson CL, Estrada C, Sverjensky DA, Cleaves HJ, Hazen RM. Adsorption of l-aspartate to rutile (α-TiO2): Experimental and theoretical surface complexation studies. *Geochimica et Cosmochimica Acta.* 2010;74(8):2356-2367.
21. Gallegos A, Wu J. Charge Regulation of Natural Amino Acids in Aqueous Solutions. *Journal of Chemical & Engineering Data.* 2020;65(12):5630-5642.
22. Kong X, Jiang J, Lu D, Liu Z, Wu J. Molecular Theory for Electrokinetic Transport in pH-Regulated Nanochannels. *The Journal of Physical Chemistry Letters.* 2014;5(17):3015-3020.
23. Ong GMC, Gallegos A, Wu J. Modeling Surface Charge Regulation of Colloidal Particles in Aqueous Solutions. *Langmuir.* 2020;36(40):11918-11928.
24. Yang J, Su H, Lian C, Shang Y, Liu H, Wu J. Understanding surface charge regulation in silica nanopores. *Physical Chemistry Chemical Physics.* 2020;22(27):15373-15380.
25. Sverjensky DA, Fukushi K. A predictive model (ETLM) for As(III) adsorption and surface speciation on oxides consistent with spectroscopic data. *Geochimica et Cosmochimica Acta.* 2006;70(15):3778-3802.
26. Sverjensky DA, Fukushi K. Anion Adsorption on Oxide Surfaces: Inclusion of the Water Dipole in Modeling the Electrostatics of Ligand Exchange. *Environmental Science & Technology.* 2006;40(1):263-271.
27. Tamura H, Mita K, Tanaka A, Ito M. Mechanism of Hydroxylation of Metal Oxide Surfaces. *Journal of Colloid and Interface Science.* 2001;243(1):202-207.
28. Akratopulu KC, Kordulis C, Lycourghiotis A. Effect of temperature on the point of zero charge and surface charge of TiO2. *Journal of the Chemical Society, Faraday Transactions.* 1990;86(20):3437-3440.
29. Loux NT. Extending the diffuse layer model of surface acidity behaviour: III. Estimating bound site activity coefficients. *Chemical Speciation & Bioavailability.* 2009;21(4):233-244.
30. Gómez-Bombarelli R, González-Pérez M, Pérez-Prior MT, Calle E, Casado J. Computational Calculation of Equilibrium Constants: Addition to Carbonyl Compounds. *The Journal of Physical Chemistry A.* 2009;113(42):11423-11428.
31. Mansoori GA, Carnahan NF, Starling KE, Leland TW. Equilibrium Thermodynamic Properties of the Mixture of Hard Spheres. *The Journal of Chemical Physics.* 1971;54(4):1523-1525.
32. Maribo-Mogensen B, Kontogeorgis GM, Thomsen K. Comparison of the Debye–Hückel and the Mean Spherical Approximation Theories for Electrolyte Solutions. *Industrial & Engineering Chemistry Research.* 2012;51(14):5353-5363.
33. Jin Z, Tang Y, Wu J. A perturbative density functional theory for square-well fluids. *The Journal of Chemical Physics.* 2011;134(17):174702.
34. Jang HM, Fuerstenau DW. The specific adsorption of alkaline-earth cations at the rutile/water interface. *Colloids and Surfaces.* 1986;21:235-257.
35. Kosmulski M. Isoelectric points and points of zero charge of metal (hydr)oxides: 50years after Parks' review. *Advances in Colloid and Interface Science.* 2016;238:1-61.

36. Lee N, Sverjensky DA, Hazen RM. Cooperative and Competitive Adsorption of Amino Acids with Ca2+ on Rutile (α-TiO2). *Environmental Science & Technology.* 2014;48(16):9358-9365.
37. Misra RP, de Souza JP, Blankschtein D, Bazant MZ. Theory of Surface Forces in Multivalent Electrolytes. *Langmuir.* 2019;35(35):11550-11565.
38. Imamura K, Kawasaki Y, Awadzu T, Sakiyama T, Nakanishi K. Contribution of acidic amino residues to the adsorption of peptides onto a stainless steel surface. *Journal of Colloid and Interface Science.* 2003;267(2):294-301.
39. Nagayasu T, Yoshioka C, Imamura K, Nakanishi K. Effects of carboxyl groups on the adsorption behavior of low-molecular-weight substances on a stainless steel surface. *Journal of Colloid and Interface Science.* 2004;279(2):296-306.
40. De Stefano C, Foti C, Gianguzza A, Sammartano S. The interaction of amino acids with the major constituents of natural waters at different ionic strengths. *Marine Chemistry.* 2000;72(1):61-76.
41. de Vos WM, Lindhoud S. Overcharging and charge inversion: Finding the correct explanation(s). *Advances in Colloid and Interface Science.* 2019;274:102040.
42. Waite JH. Mussel adhesion – essential footwork. *The Journal of Experimental Biology.* 2017;220(4):517.
43. Stewart RJ, Ransom TC, Hlady V. Natural underwater adhesives. *Journal of Polymer Science Part B: Polymer Physics.* 2011;49(11):757-771.
44. Kord Forooshani P, Lee BP. Recent approaches in designing bioadhesive materials inspired by mussel adhesive protein. *Journal of polymer science Part A, Polymer chemistry.* 2017;55(1):9-33.
45. Moulay S. Recent Trends in Mussel-Inspired Catechol-Containing Polymers. Part 1 (A Review. 2018.
46. Gulley-Stahl H, Hogan PA, Schmidt WL, Wall SJ, Buhrlage A, Bullen HA. Surface complexation of catechol to metal oxides: an ATR-FTIR, adsorption, and dissolution study. *Environmental science & technology.* 2010;44(11):4116-4121.
47. Bahri S, Jonsson CM, Jonsson CL, Azzolini D, Sverjensky DA, Hazen RM. Adsorption and Surface Complexation Study of L-DOPA on Rutile (α-TiO2) in NaCl Solutions. *Environmental Science & Technology.* 2011;45(9):3959-3966.
48. Krohn JE, Tsapatsis M. Phenylalanine and Arginine Adsorption in Zeolites X, Y, and β. *Langmuir.* 2006;22(22):9350-9356.

Molecular thermodynamics for amino-acid adsorption at inorganic surfaces

Alejandro Gallegos and Jianzhong Wu*

Department of Chemical and Environmental Engineering, University of California, Riverside, CA 92521, USA

Abstract

The interaction of polypeptides and proteins with an inorganic surface is intrinsically dependent on the interfacial behavior of amino acids and sensitive to solution conditions such as pH, ion type, and salt concentration. A faithful description of amino-acid adsorption remains a theoretical challenge from a molecular perspective due to the strong coupling of local thermodynamic nonideality and inhomogeneous ionization of both the adsorbate and substrate. Building upon a recently developed coarse-grained model for natural amino acids in bulk electrolyte solutions, here we report a molecular theory to predict amino-acid adsorption on ionizable inorganic surfaces over a broad range of solution conditions. In addition to describing the coupled ionization of amino acids and the underlying surface, the thermodynamic model is able to account for both physical binding and surface associations such as hydrogen bonding or bidentate coordination. It is applicable to all types of natural amino acids regardless of the solution pH, salt type and concentration. The theoretical predictions have been validated by extensive comparison with experimental data for the adsorption of acidic, basic, and neutral amino acids at rutile (α-TiO_2) surfaces.

Keywords:

Surface adhesion, charge regulation, classical density functional theory

* Corresponding author. E-mail addresses: jwu@engr.ucr.edu

1. Introduction

Understanding the interaction of amino acids with inorganic surfaces is a prerequisite for studying the interfacial behavior of polypeptides and proteins under various solution conditions. By reducing the complexity of the polymeric systems to their building blocks, we may identify key components of surface forces dictating both the adsorption and functionality of biomolecules at the interface[1-3]. However, despite its simplicity in comparison with proteins, the adsorption of amino acids in aqueous solutions is not yet fully understood from a molecular perspective[4]. The difficulty arises not only from multifaceted interactions between amino acids and an inorganic surface but also from the variation of both the surface charge and the degree of ionization of the functional groups in response to the changes in solution conditions such as pH, ion type, and salt concentration.

In addition to amine and carboxyl groups, natural amino acids consist of different side chains that vary in size and hydrophobicity. The diverse characteristics of these functional groups leads to complex interactions with inorganic surfaces in an aqueous medium. Conventionally, the surface forces are described in terms of electrostatic interactions, van der Waals and hydrophobic attractions, hydration forces, and various forms of surface association or chemical bonding. The intricate interplay of these physical and chemical interactions is coupled with protonation/deportation and multi-body correlations due to the inhomogeneous distributions of ionic species (and solvent molecules) near the surface. For most systems of practical interest, a first principles approach to predicting such interactions is beyond the reach of current computation capabilities. As a result, coarse-grained models may serve as a reasonable starting point to describe the adsorption and surface behavior.

A number of experimental techniques can be used to study the adsorption of amino acids at inorganic surfaces[5-8]. One such technique is infrared (IR) spectroscopy, which provides valuable insight into the mechanisms of amino-acid adsorption through the comparison of the spectra of adsorbed species versus that in the bulk solution. For example, IR measurements revealed glutamic acid and aspartic acid binding with γ-Al_2O_3 through oxygen atoms from one or both carboxyl groups[9]. An indirect way to measure amino-acid adsorption is by monitoring its concentration in the bulk phase[7,10-13]. The adsorption isotherm, i.e., the amount of amino acid adsorbed on the surface as a function of the *equilibrium* concentration in the bulk solution, can be determined from the reduction of the amino-acid concentration in the bulk solution. Radiotracer experiments are applicable to adsorption from dilute solutions whereby the depletion method is not possible[14]. With the help of a semi-empirical model such as the Langmuir equation, the adsorption isotherms provide valuable insight into the strength of surface binding and the maximum occupancy of amino acids. Whereas conventional adsorption models may be employed as a benchmark to compare the adsorption of amino acids at different surfaces, the model parameters are typically dependent on solution conditions thus have little predictive capability.

Complementary to experimental investigations, molecular modeling offers valuable details to bridge the knowledge gap between microscopic and macroscopic observations. Whereas atomistic models can be used to describe amino-acid adsorption through molecular dynamics (MD) simulation[15-17], coarse-grained models are often more convenient for the development of analytical methods. By capturing the essential features of intermolecular interactions and surface forces, coarse-grained models are able to provide quantitative predictions in good agreement with experimental observations. For example, Vlasova and Golovkova studied the adsorption of basic amino acids to highly dispersed silica using a surface-complexation model that describes the

amino-acid molecules at the silica surface through a Stern model of the electric double layer[18]. Two parameters were used for each amino acid, *viz*., the equilibrium constants governing the reaction of amino acids with a neutral or a negatively charged surface. With the assumption that these parameters were dependent upon the salt concentration but insensitive to the pH, the theoretical predictions of adsorption isotherms were found in quantitative agreement with experimental data. Similarly, Jonsson et al. proposed a surface-complexation model to describe the adsorption isotherms of L-aspartate and L-glutamate to a rutile surface at various solution conditions[19,20]. They proposed a reaction scheme that involved association of the acidic amino acids with the rutile surface through the binding of either one or both carboxyl groups to one or four surface titanium sites, respectively. Like the Langmuir adsorption isotherm, the surface-complexation models neglect thermodynamic non-ideality due to excluded volume effects and electrostatic correlations that are important in describing the charge regulation of amino acids both in the bulk solution and near the surface.

In order to accurately describe the adsorption of amino acids to inorganic surfaces, we must account for thermodynamic non-ideality due to interactions between amino acids and all ionic species in the solution. In addition, it is essential to capture the charge behavior of amino acids as well as the ionization of the inorganic surfaces that play a significant role in the adsorption process. In our previous work, we developed a coarse-grained model for aqueous solutions of amino acids that appropriately takes into account bulk interactions[21]. The thermodynamic model provides a faithful description of the charge behavior of amino acids as a function of pH and solution conditions. In addition, we proposed a coarse-grained model to describe the charge regulation of various ionizable surfaces by an explicit consideration of the inhomogeneous ion distributions and surface reactions[22-24]. Herein, we combine these models to examine the adsorption behavior of

amino acids at the rutile (α-TiO_2) surface. The molecular-thermodynamic model allows us to predict the adsorption of various amino acids in response to the changes in solution conditions. This predictive model fills the gap between phenomenological models to describe the adsorption of amino acids and all-atom or first-principles simulations. Importantly, the theoretical procedure may provide a foundation for future studies of the interaction of polypeptides and proteins with various inorganic surfaces under diverse solution conditions.

2. Thermodynamic Model and Methods

2.1 *A coarse-grained model for amino-acid adsorption*

In this work, we are interested in developing a coarse-grained model applicable to amino-acid adsorption at an ionizable surface over a broad range of solution conditions. Toward that end, we employ an augmented primitive model (APM) that explicitly accounts for the different charged states of natural amino acids[21]. Due to the variation of hydration structure in response to the deprotonation or protonation of ionizable sites, each amino-acid molecule has a unique hard-sphere diameter σ_i and valence Z_i in different charged states.

Figure 1 shows a schematic representation of amino acids near an organic surface as described by the APM model. As in the primitive model (PM) that is conventionally used to describe the thermodynamic properties of aqueous electrolyte solutions, all amino acids and ionic species are represented by charged hard spheres and the solvent by a dielectric continuum of relative primitivity $\varepsilon_r = 78$, which corresponds to that for liquid water at the ambient condition. Because of ionization, each amino acid exists as a mixture of molecules in discrete integer-value charge states. In addition to the variation of the valence in response to pH changes, the augmented aspect of the primitive model is the inclusion of various well-recognized but poorly-understood water-mediated interactions among amino acids and other ionic species in the solution as well as

their short-range interactions with the surface. In this work, such interactions are described through a square-well model. While the phenomenological description neglects atomic details and the anisotropic nature of amino-acid molecules, it provides a flexible framework to quantify the interfacial behavior of various natural amino acids in aqueous solutions by treating the square-well width and attraction energy as adjustable parameters. We demonstrated in our previous work that the augmented model is able to reproduce both the titration behavior and the thermodynamic properties of amino-acid solutions in good agreement with experimental observations[21].

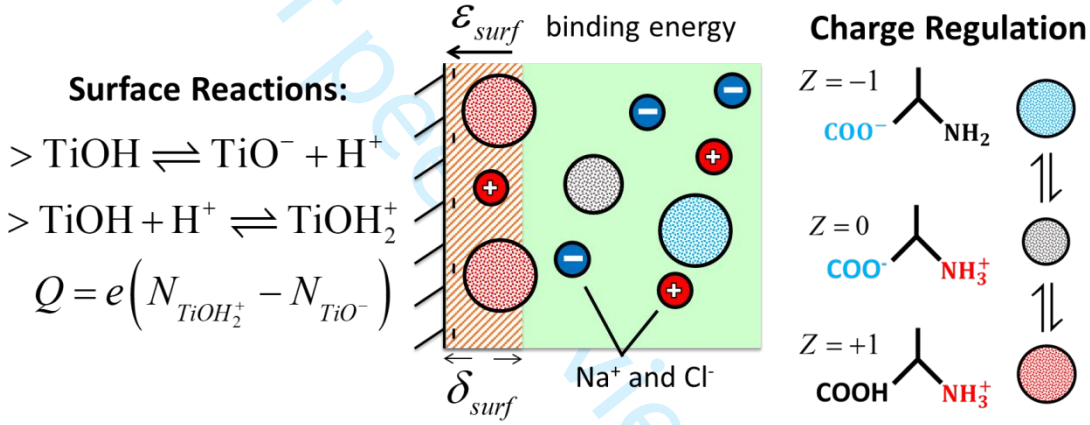

Figure 1. A coarse-grained model for the adsorption of natural amino acids on a rutile surface. In an aqueous solution, an amino-acid molecule may exist in different charged states dependent on the solution condition. The rutile surface may develop a net charge through deprotonation or protonation of the hydroxyl sites.

The coarse-grained model can be similarly applied to the adsorption of amino acids at an inorganic surface. In this case, the surface is represented by a hard wall with the charge density determined from the dissociation equilibrium of ionizable sites and ionic distributions self-consistently[22-24]. In addition to the electrostatic interactions and excluded volume effects, the surface interacts with amino acids through semi-empirical short-range interactions (e.g., hydrophobic attraction and hydrogen bonding). As in the PM description of electrolyte solutions,

the van der Waals attraction is relatively insignificant in comparison with other forms of surface forces. Because our model accounts for ionization and the electrostatic charges of amino-acid molecules explicitly, we neglect the polarity effects on intermolecular and surface interactions. Our results suggest that the remanent electrostatic effects are effectively accounted for by short-range bindings. For simplicity, we fix the range of the short-range interaction between the surface and all amino acids at δ_{surf} = 0.4 nm from the edge of the hard wall (see Figure 1). The choice of four angstroms is somewhat arbitrary in that a shift of the range of attraction can always be compensated by changing the energy parameter. Nevertheless, the chosen value appears reasonable from physical considerations because both hydrophobic interactions and hydrogen bonding are most significant when the amino acid is in intimate contact with the surface. It should be noted that δ_{surf} is immaterial to the identity of amino acids.

According to APM, the external potential due to the inorganic surface is expressed as

$$V_i^{ext}(z) = \begin{cases} \infty & z < \sigma_i / 2 \\ -\varepsilon_{surf,i} & \sigma_i / 2 \le z \le \delta_{surf} \\ 0 & else \end{cases} . \quad (1)$$

In Eq. (1), the first line on the right accounts for the hard-wall repulsion, which limits the access of a chemical species (viz., ions and amino acids) to the solid phase beyond the point of contact; and the second line accounts for the short-range attraction. The latter is represented by a square-well potential with a constant energy in the immediate vicinity of the surface. Because of the excluded-volume effects, the closest distance for an amino acid from the surface depends on its hard-sphere diameter. As a result, the range of non-electrostatic surface attraction is different for different amino acids. On the other hand, the square-well energy, ε_{surf}, accounts for specific binding of an amino acid molecule with the surface. We expect that this parameter should be

relatively insensitive to the changes in solution conditions (e.g., salt concentration), but may vary with temperature, because it reflects the local properties of the underlying chemical species. The results here are reported for T=298.15 K. The surface energy may also be used to account for adsorption of amino acids due to specific chemical bonding with the surface. To a certain degree, our description of amino-acid binding with an inorganic surface is equivalent to surface complexation modeling mentioned above[25,26]. One benefit of our thermodynamic approach is that it takes into account the solution effects on amino-acid adsorption.

2.2 *Charge regulation for inorganic surfaces*

In an aqueous solution, inorganic surfaces are typically terminated with hydroxyl groups due to the chemical adsorption of water molecules[27]. The deprotonation or protonation of these functional groups leads to a surface charge that can be regulated by adjusting the solution pH or salt concentration. Even for the same surface, the charge density may differ in both magnitude and sign depending on the solution conditions.

Due to its broad use as bioimplants, titanium dioxide is commonly used as a model inorganic material for studying amino-acid adsorption. In particular, experimental studies are mostly focused on rutile (100) and (110) surfaces as single crystals with these orientations are readily available. For a rutile surface, the deprotonation and protonation reactions are given by[28]

$$\text{-TiOH} \rightarrow \text{-TiO}^- + \text{H}^+, \tag{2}$$

$$\text{-TiOH} + \text{H}^+ \rightarrow \text{-TiOH}_2^+. \tag{3}$$

The equilibrium constants for these two reactions, K_D and K_P, respectively, are connected with the solution $\text{pH} = -\log a_{H^+}$ and the activities of the surface sites:

$$K_D = \frac{N_{TiO^-}}{N_{TiOH}} \frac{\gamma_{TiO^-}}{\gamma_{TiOH}} a_{H^+}, \tag{4}$$

$$K_P = \frac{N_{TiOH_2^+}}{N_{TiOH}} \frac{\gamma_{TiOH_2^+}}{\gamma_{TiOH}} \frac{1}{a_{H^+}} \tag{5}$$

where N_i refers to the number of surface site *i* per unit area, and γ_i is the activity coefficient of the corresponding surface site.

The activity coefficient of each surface group accounts for its physical interactions with the environment[29]. In this work, we assume that the ratio of the activity coefficients for each surface group in its different charge states to be governed by the local electrostatic potential (i.e., the surface potential, ψ_s). Thus, the surface reaction equilibrium can be re-expressed in terms of apparent equilibrium constants, K'_D and K'_P,

$$K'_D = K_D \frac{\gamma_{SOH}}{\gamma_{SO^-}} = K_D \exp\left(\beta e \psi_s\right), \tag{6}$$

$$K'_P = K_P \frac{\gamma_{SOH}}{\gamma_{SOH_2^+}} = K_P \exp\left(-\beta e \psi_s\right). \tag{7}$$

The surface charge density is related to the total number density of the site and can be determined from the mass and charge balance:

$$N_{sites} = N_{SOH} + N_{SO^-} + N_{SOH_2^+}, \tag{8}$$

$$Q = -e\left(N_{SO^-} - N_{SOH_2^+}\right) \tag{9}$$

where N_{sites} refers to the total number of surface groups per unit area, *e* is the elementary charge, and Q is the surface charge density.

The combination of Eqs. (4-9) leads to an explicit expression for the surface charge density in terms of the total number of available sites per unit area, the apparent equilibrium constants, and the proton activity:

$$Q = -e\,N_{sites}\,\frac{K_D'/a_{H^+} - K_P'\,a_{H^+}}{1 + K_D'/a_{H^+} + K_P'\,a_{H^+}}. \tag{10}$$

Since the apparent equilibrium constants change with the surface potential, the surface charge density depends on the inhomogeneous ion distributions near the surface. As a result, the charge regulation of amino acids is more complex than that in the bulk solution due to the interfacial behavior of all charged species playing a key role in determining the local solution condition.

2.3 *Ionization of amino acids in an inhomogeneous environment*

Each amino acid molecule consists of a carboxyl group and an amine group which can be deprotonated and protonated, respectively, at suitable solution conditions. Neutral amino acids are referred to as those that do not contain any ionizable functional groups in the side chain. On the other hand, acidic and basic amino acids contain an additional functional group in their side chains that can be deprotonated and protonated, leading to an additional negative and positive charge, respectively. As a result of the acid-base equilibrium, amino acids exist in multiple charged states dependent on the pH and other solution conditions.

For each amino acid, the acid-base equilibrium can be described in terms of multi-step protonation reactions

$$\mathrm{A_{i-1}} + \mathrm{H^+} \leftrightarrow \mathrm{A_i} \tag{11}$$

where $\mathrm{A_i}$ refers to the amino acid in a given charged state. The amino-acid valence satisfies $Z_{A_i} = Z_{A_0} + i$ with $Z_{\mathrm{A_0}}$ being the charge for the amino acid in its fully deprotonated state. For a neutral or basic amino acid, $Z_{\mathrm{A_0}} = -1$; while an acidic amino acid has a valence of -2 in its fully deprotonated state. Accordingly, in the fully protonated state, each neutral or acidic amino acid has a valence of +1, and each basic amino acid has a valence of +2.

Similar to that in the bulk solution, the equilibrium constant for the protonation of amino acids in an inhomogeneous environment (viz., near the surface) is related to the local solution composition and activity coefficients

$$K_i^T = \frac{\rho_{A_i}(z)}{\rho_{A_{i-1}}(z)} \frac{\gamma_{A_i}(z)}{\gamma_{A_{i-1}}(z)} \frac{1}{a_{H^+}} \tag{12}$$

where K_i^T represents the equilibrium constant for the amino acid in charge state i, $\rho_i(z)$ is the number density of species i at perpendicular distance z from the surface, and γ_i is its local activity coefficient. The equilibrium constant is a thermodynamic quantity defined by the change in the chemical potentials of reactants and products at their corresponding reference states, i.e., each species in an ideal solution at unit molar concentration[30]. These values were obtained in our previous work based off correlations with experimental data for all natural amino acids in bulk NaCl solutions[21]. The activity coefficients account for the effect of solvent-mediated interactions among all chemical species in the solution.

Within the augmented primitive model (APM), the local activity coefficient can be expressed as

$$k_B T \ln \gamma_i = \mu_i^{ex} = \mu_i^{hs} + \mu_i^{sw} + \mu_i^{el} + \psi Z_i e + V_i^{ext} \tag{13}$$

where μ_i^{ex} stands for the local excess chemical potential, *i.e.*, deviation from the chemical potential of species i in an ideal solution; k_B is the Boltzmann constant, and T is the absolute temperature. μ_i^{hs}, μ_i^{el}, and μ_i^{sw} are contributions to the local excess chemical potential due to hard-sphere repulsion, electrostatic correlation, and solvent-mediated interactions, respectively. The last two terms, V_i^{ext} and ψ, are the external potential due to the interface (e.g., hard wall and specific

binding to the surface) and the local electrostatic potential, respectively. The expression for each contribution has been discussed previously and can be found in Supporting Information[31-33].

2.4 *Classical Density Functional Theory*

Classical density functional theory (cDFT) provides a generic mathematical procedure to describe the inhomogeneous distributions of ionic species including amino acids near inorganic surfaces. At a given temperature T and the bulk densities of all ionic species $\{\rho_i^b\}$, cDFT predicts the local density, $\rho_i(z)$, of each species by minimizing the grand potential

$$\Omega = F + \sum_i \int \left[V_i^{ext}(z') - \mu_i \right] \rho_i(z') dz' \tag{14}$$

where V_i^{ext} and μ_i are the external potential and the chemical potential of species i, respectively, and F denotes the total intrinsic Helmholtz energy. The latter consists of an ideal-gas contribution and the excess arising from intermolecular interactions. Similarly, the chemical potential is composed of an ideal part, which is directly related to the number density of the species, and an excess part as discussed in the prior section.

For systems considered in this work, the intermolecular interactions include the hard-sphere repulsion, electrostatic correlations, solvent-mediated interactions, and direct coulombic interactions. As the chemical potential is uniform throughout the system, any change in the local environment directly influences the local densities of all species as predicted by the Euler-Lagrange equation:

$$k_B T \ln \rho_i^b + \mu_i^{ex,b} = k_B T \ln \rho_i(z) + \mu_i^{ex,\text{int}}(z) + \psi(z) Z_i e + V_i^{ext}(z). \tag{15}$$

The left side of Eq. (15) corresponds to the chemical potential of species i in the bulk, whereas the right side is that at position z in the inhomogeneous fluid (i.e., near the interface). Similar to that in the bulk solution, the excess chemical potential $\mu_i^{ex,int}$ accounts for intermolecular interactions

other than the direct Coulomb contribution. The latter is related to the mean electrostatic potential, ψ, which includes contributions from Coulomb interactions between all ionic species and the surface. The last term on the right side of Eq. (15), V_i^{ext}, denotes the non-electrostatic interactions with the surface, i.e., the hard-wall and short-range attraction as given by Eq. (1). It is worth noting that the chemical equilibrium between the different electrostatic states of the amino acid near the surface is naturally satisfied within our cDFT calculations.

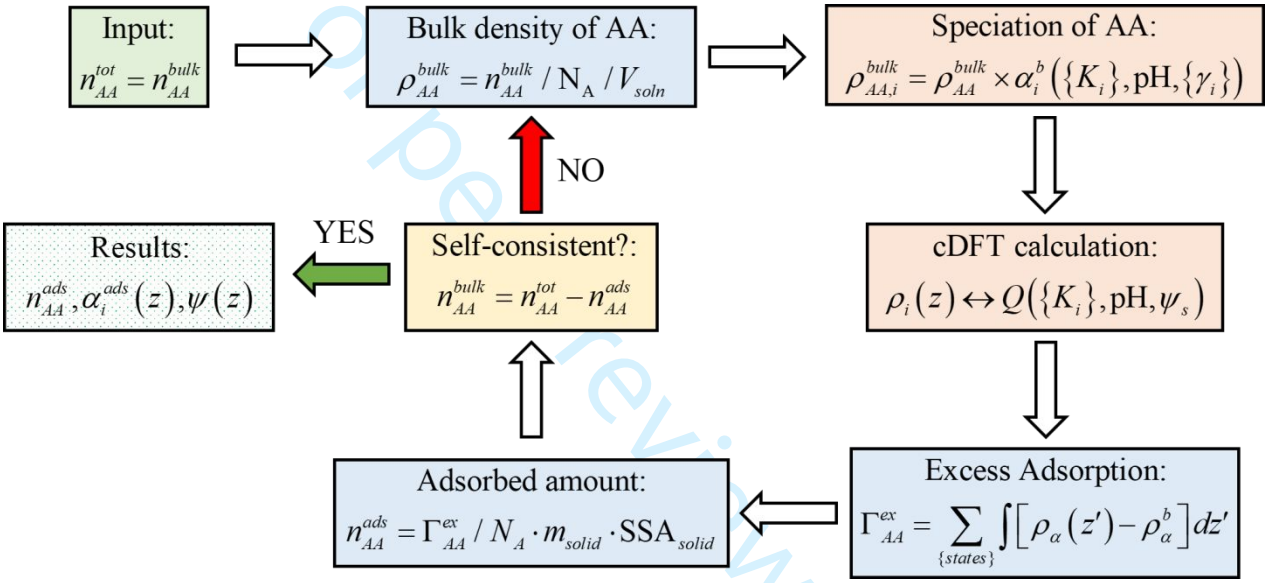

Figure 2. A flowchart of the computational procedure to determine the adsorption of amino acids on an inorganic surface. In consistent with experimental measurements of adsorption isotherms, each cDFT calculation is carried out at a fixed temperature, volume, and the total moles of amino acid n_{AA}^{tot} in the system.

To facilitate direct comparison of the theoretical results with experimental data, we must perform the cDFT calculations for the adsorption of amino acids at an inorganic surface at a fixed total number of amino-acid molecules in the solution. Figure 2 presents a flowchart of our calculation procedure. The total amount of amino acid in the solution includes contributions from both the adsorbed amount on the surface as well as that in the bulk solution, i.e., $n_{AA}^{tot} = n_{AA}^{bulk} + n_{AA}^{ads}$.

However, the cDFT calculation must be performed at a fixed bulk chemical potential, i.e., the bulk density of each species must be known *a priori*. To convert the moles of amino acid in the solution to a bulk density, we must know the solution volume (V_{soln}). We can then relate the total number of moles of the amino acid to its corresponding bulk density by $\rho_{AA}^{bulk} = n_{AA}^{bulk} / N_A / V_{soln}$, where N_{A} is Avogadro's number. Because we explicitly consider the chemical equilibrium between the different ionization states of each amino acid, we must also determine the bulk density for the amino acid at each ionization state. The degree of dissociation at state i is defined by $\alpha_i = \rho_{A_i} / \sum_j \rho_{A_j}$, where the summation extend over all possible charged states of the amino acid. By coupling the degree of ionization with the expressions for protonation/deprotonation equilibrium, we can determine the relative presence of each charged state for the amino acid from

$$\alpha_i = \frac{a_{H^+}^i \prod_{j=1}^{i} K'_j}{1 + \sum_{j=\{states\}} a_{H^+}^j \prod_{k=1}^{j} K'_k} \tag{16}$$

where $K'_j = K_j^T \gamma_{A_{j-1}} / \gamma_j$ is the apparent equilibrium constant defined by the thermodynamic equilibrium constant and the ratio of the bulk activity coefficients.

Eq. (16) can be solved numerically by using known equilibrium constants for different functional groups of the amino acid and the augumented primitive model (APM) to account for thermodynamic non-ideality. Once the bulk density of the amino acid at each charged state has been determined from $\rho_{AA_i}^{bulk} = \rho_{AA}^{bulk} \alpha_i$, cDFT calculation is then performed to determine the adsorption of the amino acid at the inorganic surface. The chemical equilibrium for the protonation/deprotonation of amino acids in the inhomogeneous environment will be automatically satisfied as shown by Eq. (15). During the cDFT calculations, we determine the

density profiles of the amino-acid molecules in different charged states along with the distributions of salt ions. The charge density of the inorganic surface can be calculated from the condition of charge neutrality as shown in Eq. (9). The surface excess for each amino acid, i.e., the amount adsorbed at the surface, is given by

$$\Gamma_{AA}^{ex} = \sum_{\{states\}} \int \left[\rho_\alpha (z') - \rho_\alpha^b \right] dz' . \tag{17}$$

Given the total mass (m_{solid}) and the specific surface area (SSA) of the solid, the excess adsorption can be related to the total adsorbed amount by

$$n_{AA}^{ads} = \Gamma_{AA}^{ex} / N_A \cdot m_{solid} \cdot \text{SSA}_{solid} . \tag{18}$$

As mentioned above, experimental measurements of adsorption isotherms are often reported in terms of the total moles of amino acid in the solution. The sum of amino acids in the bulk and that at the surface must be equal to the total moles in the solution. In our cDFT calculations, we iterate the cDFT calculations with the mole amount in the bulk given by $n_{AA}^{bulk} = n_{AA}^{tot} - n_{AA}^{ads}$ and solve for n_{AA}^{ads} from Eq. (18) until the quantity is converged. After convergence, we can make direct comparison of the theoretical results with experimental data for the adsorbed amount of each amino acid given that the total amino acid in the solution is fixed.

3. Results and Discussion

In the following, we provide 3 case studies to illustrate the application of our coarse-grained model to describe the effects of solution conditions on the adsorption of amino acids on different inorganic surfaces. We first consider the charge regulation of rutile in different salt solutions. Rutile can be either positively or negatively charged depending upon the solution pH. Next, we investigate the adsorption isotherms on rutile (110) surface for the three charge classes of natural amino acids: acidic, basic, and neutral. We find that the adsorption of these amino acids

is highly dependent upon pH, amino acid concentration, and salt concentration in the bulk solution. Due to the protonation/deprotonation of both the amino acid molecules and the rutile surface, the adsorption isotherm typically shows a maximum at an intermediate pH value that is dependent upon the salt type and concentration. In all cases, we find that our coarse-grained model performs well in capturing the adsorption behavior of natural amino acids in different solution conditions.

3.1 *Surface charge of rutile in aqueous NaCl and $CaCl_2$ solutions*

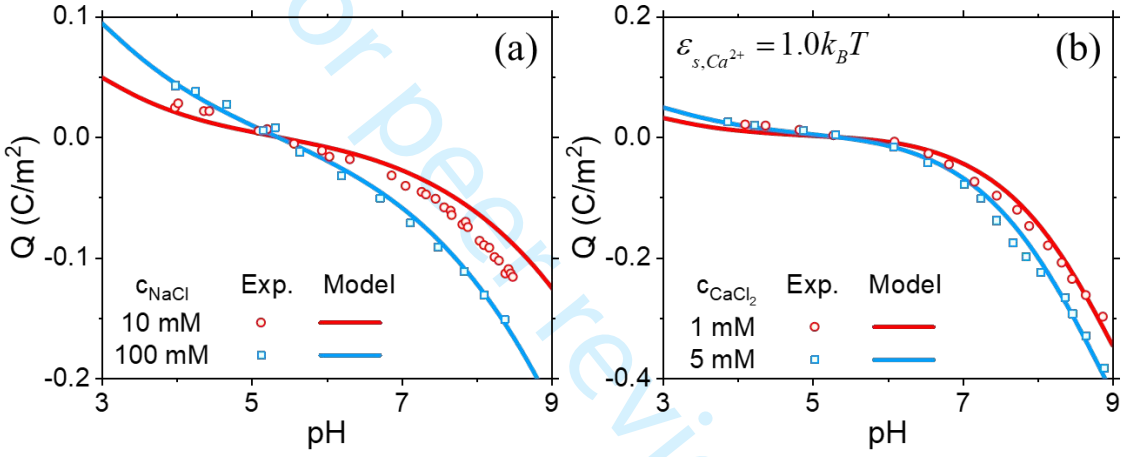

Figure 3. The surface charge density of rutile as a function of pH in (a) NaCl solution and (b) $CaCl_2$ solution from experiment[19,34] (symbols) and from the prediction of the coarse-grained model (lines). The surface site density is fixed at 3 nm^{-2} in agreement with Bahri et al.[19]. The deprotonation and protonation constants are pK_D=6.5 and pK_P=-4.1, respectively.

Charge regulation is important for understanding the adsorption of amino acids at rutile (and other inorganic) surfaces as the adsorption is highly sensitive to electrostatic interactions. Figure 3 shows the surface charge density of rutile in sodium chloride and calcium chloride aqueous solutions at two representative salt concentrations. By employing the augmented primitive model (APM) for aqueous electrolytes, we can describe the surface charge at different pH and salt concentrations by using only the thermodynamic equilibrium constants for protonation

and deprotonation. These two constants are inherently coupled with the isoelectric point of the surface which can be related by $pI = (pK_D - pK_P)/2$. We set the isoelectric point to pI=5.3 consistent with previous experimental findings[35]. Based on this, the deprotonation and protonation constants were determined to be pK_D = 6.5 and pK_P = -4.1, respectively. The surface charge is highly dependent on pH and, to a lesser extent, on sodium chloride concentration. The addition of salt ions to the solution reduces the electrostatic repulsion between surface sites leading to an increase in the surface charge at a fixed pH[17]. APM slightly overestimates electrostatic repulsion between the surface sites as shown by the underestimation of the surface charge at 10 mM. A more sophisticated approach to describe the surface reactions (e.g., multi-site or ion-complexation) could lead to more accurate prediction of the surface charge regulation. As can be seen from Figure 3, the rutile surface is positively charged at low pH (i.e., below its isoelectric point) and negatively charged at high pH. The regulation of the surface charge provides a convenient way to promote or inhibit the adsorption of amino acids or charged organic molecules. We see that APM provides a quantitative description of the effects of the monovalent electrolyte on the surface charge of rutile. A good agreement of the theoretical prediction and experiment was also found for other inorganic surfaces[22,24].

We next consider the surface charge of rutile in calcium chloride solutions. As shown in Figure 3b, the deprotonation of the rutile surface (i.e., increases in negative charge) is less dependent on pH in the presence of calcium ions. The trend is noticeable despite the fact that the concentration of calcium ions is one order of magnitude smaller than that of sodium ions (e.g., 1 mM $CaCl_2$ vs. 10 mM NaCl). Such behavior can be attributed to the stronger electrostatic binding between the negatively charged surface sites and the divalent cation. On the other hand, when rutile is positively charged, the influence of the cation valence is negligible as it is the monovalent

chloride ions dictating the surface charge density. To match the experimental data for rutile in the presence of calcium chloride, we used the same equilibrium constants determined for rutile in sodium chloride solutions. However, this led to a consistent underestimation of the surface charge above the isoelectric point. Previous studies have demonstrated the importance of calcium binding to surface hydroxyl sites beyond electrostatic attraction[36]. It has also been suggested that the hydration of the calcium ion near the surface is different from that in the bulk[37]. To account for such effects, we introduced a short-range attraction of magnitude ε_{surf} = 1.0 k_BT between the calcium ions and the rutile surface to mimic this non-electrostatic binding behavior. The inclusion of this short-range attraction leads to a perfect description of the ionization behavior of rutile in the presence of calcium chloride.

3.2 *Adsorption of acidic amino acids to rutile*

The adsorption of amino acids at inorganic surfaces is complicated by the fact that both the amino acid and surface are ionizable and that the surface forces are highly sensitive to the solution pH and local ion concentrations. Due to competing electrostatic interactions, the adsorption isotherm is often nonmonotonic with respect to pH and shows a strong dependence on solution conditions (e.g., salt type and concentration). To elucidate, Figure 4 presents the adsorption of glutamic acid and aspartic acid at a rutile surface versus pH at several sodium chloride and amino acid concentrations. The adsorption of both acidic amino acids shows a maximum near the pK_a value of the amino-acid side chain. At this condition, approximately 50% of the acidic amino acids carry a negative charge. A reduction of the pH below the pK_a would shift the equilibrium to the neutral state while an increase in pH would result in the amino acids existing predominately in their negatively charged state. Meanwhile, the rutile surface exhibits a positive charge below its isoelectric point of pI=5.3, which leads to a pH window where the adsorption is favored by the

electrostatic interaction between the surface and the amino acid. Surprisingly, significant adsorption is observed even at pH=9 where there is a strong electrostatic repulsion between the acidic amino acids and the negatively charged surface. In this case, the adsorption can be attributed to hydrogen bonding between the carboxyl groups from the amino acids and the surface hydroxyl sites[38,39]. Such interaction can be modeled through a square-well potential between the amino acid and the surface, irrespective of the charge status. We determined the fitting parameter to be ε_{surf} =9.6 k_BT based off a comparison with the experimental adsorption data for 0.5 mM amino acid and 100 mM sodium chloride solution. Due to similarities in the chemical structure of both acidic amino acids, it is expected that the two will interact similarly with the rutile surface. Therefore, we did not distinguish the surface binding energy between the two amino acids which, as demonstrated by Figure 4, was found to be satisfactory.

As expected, the solution condition has an important effect on the adsorption of acidic amino acids at the rutile surface. In general, the adsorbed amount increases with the total concentration of amino acid in the solution. For example, the mean lateral separation between glutamic acid on the rutile surface at pH 3 decreases from approximately 3 nm (~0.2 μmol/m^2) to 1 nm (~1.52 μmol/m^2) when the concentration of glutamic acid is increased from 0.1 mM to 2.0 mM. Such effect is most noticeable at low pH because the opposite surface charge leads to a stronger driving force for the adsorption. While the amino-acid concentration has little effect on the solution pH at which the maximum in adsorption occurs, the salt concentration results in a notable shift in the pH at which the adsorption is maximized. The variation of the salt concentration will also influence the adsorption of charged amino acids because of the electrostatic screening effect.

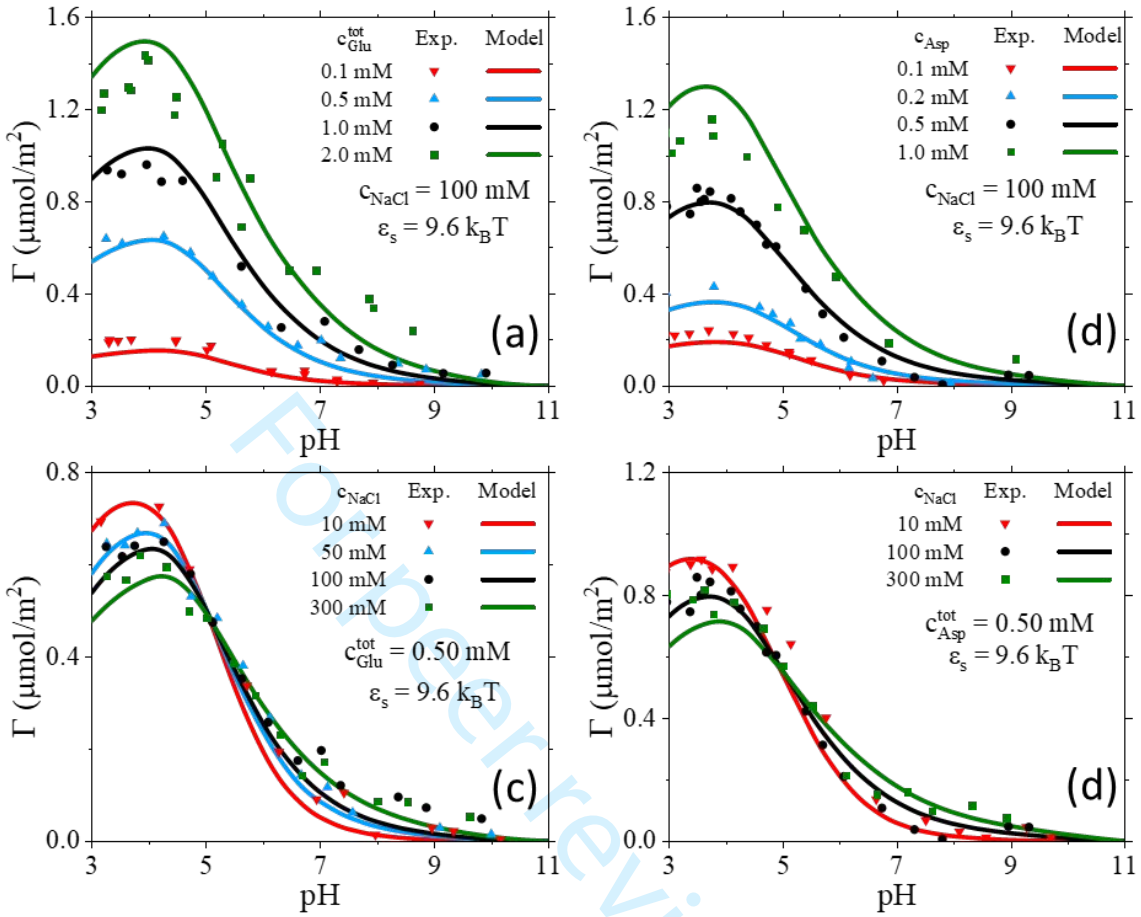

Figure 4. The pH-dependent adsorption of glutamic acid and aspartic acid on the rutile surface at (a and b) various total concentrations of amino acids in a 100 mM aqueous NaCl solution and (c and d) several NaCl concentrations in a 0.50 mM aqueous amino acid solution. The symbols are from experiment[19], and the lines are predictions of the coarse-grained model.

It has been well documented that the addition of salt ions to the solution will promote ionization of the inorganic surface by decreasing the electrostatic repulsion between the surface sites (as shown previously in Figure 3). However, it is not clear how the distribution of charged states for the amino acid is affected by the increase in salt concentration. While the ionized forms of the amino acid would be typically favored by increasing the salt concentration in the bulk solution, the reduced Coulomb interaction with the surface sites may be more impactful on amino-acid speciation. Since an increase in the salt concentration shifts the maximum adsorption to a

higher pH (i.e., the chemical equilibrium shifts to the negatively charged state of the amino acid), we expect that, at a fixed pH, the addition of salt inhibits amino acids in the ionized state. This is because a weaker interaction with the positively charged surface by the negatively charged amino acid reduces the preference of the amino acid in its anionic state.

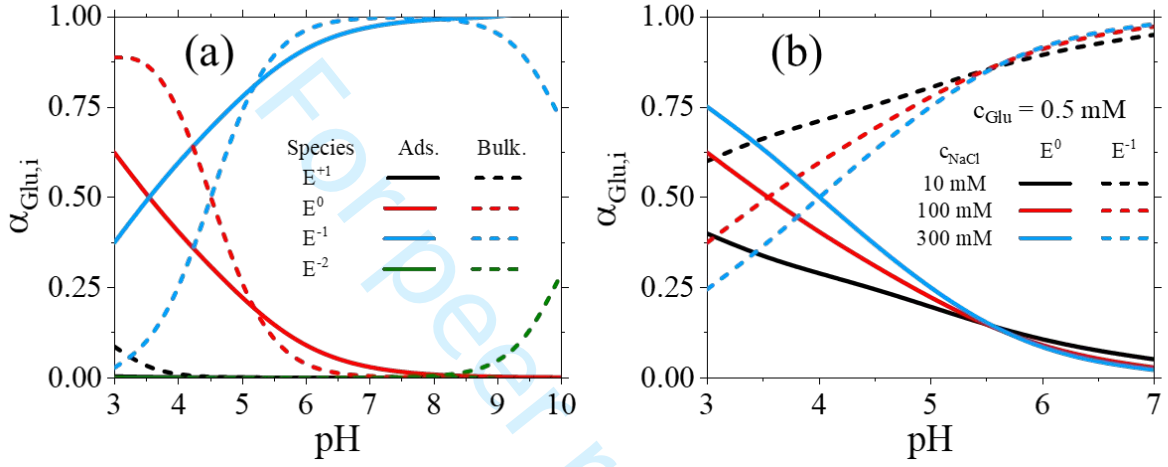

Figure 5. (a) The pH-dependent speciation of glutamic acid at the rutile surface and in the bulk solution. The total concentration of glutamic acid is 0.5 mM, and the NaCl concentration is 100 mM. (b) Speciation of adsorbed glutamic acid into its two predominant states, neutral and negatively charged, in the pH range of 3 to 7 at three NaCl concentrations (10, 100, and 300 mM).

The interfacial behavior of amino acids at inorganic surfaces are dependent on their ionization states near the surface. In most cases, the dominate charge state at the surface is significantly different from that in the bulk solution due to the selective interactions of the surface with amino acid molecules. To demonstrate this, we show in Figure 5a the pH-dependent speciation of glutamic acid in the bulk solution and on the rutile surface in 100 mM sodium chloride solution. At low pH, the amino acid is dominated by its negatively charged state due to strong Coulomb interactions with the positively charged surface sites on rutile while the amino acid mostly exists in its neutral state in the bulk solution (i.e., far from the surface). There is a

small reversal in this trend as the pH is increased because the rutile surface transitions to negatively charged and repulses the anionic state of the amino acid. At higher pH, the monovalent anionic state is maintained somewhat more than that in the bulk solution to avoid the repulsion between the negatively charged surface and amino-acid molecules in the divalent anionic state. Based off these results, it also becomes clear why there is a maximum in the adsorption at low pH seen in Figure 4. While the surface has more positive charge as pH falls, it adsorbs less amino acid even though it is negatively charged. This interplay between a stronger electrostatic attraction but a lower concentration of amino acids in the anionic state leads to the maximum adsorption in responding to the pH changes. Although the positively charged surface promotes the ionization of the acidic amino acid relative to the bulk solution, the increased electrostatic force is insufficient to compensate the reduction in the concentration of a negatively charged amino acid.

Figure 5b shows the influence of salt concentration on the speciation of the adsorbed amino acid molecules in neutral and negatively charged states. It is clear that the salt concentration plays a key role on speciation at low pH where the adsorption is mostly driven by electrostatic forces. At low pH, an increase in the salt concentration disfavors the presence of the amino acid in the negatively charged state. Interestingly, an opposite trend is observed as the salt concentration in the bulk solution rises[40]. In the former case, the addition of salt weakens the electrostatic attraction between the rutile surface and amino acid molecules (*viz*. through the reduction of the mean electrostatic potential). The electrostatic interaction is responsible for the increased population of the anionic state near the surface while the bulk solution is dominated by amino-acid molecules in the neutral state. The increase in the salt concentration reduces the mean electrostatic potential at the surface leading to a reduction of the local concentration of the amino acid in the negatively charged state. At these conditions (e.g., low pH and small salt concentration), the ionic excluded-

volume effects and electrostatic correlations are relatively insignificant in the ionization behavior of the acidic amino acid. Therefore, an accurate description of charge regulation for both the amino acid and the surface is essential for understanding the adsorption of amino acids at the rutile surface.

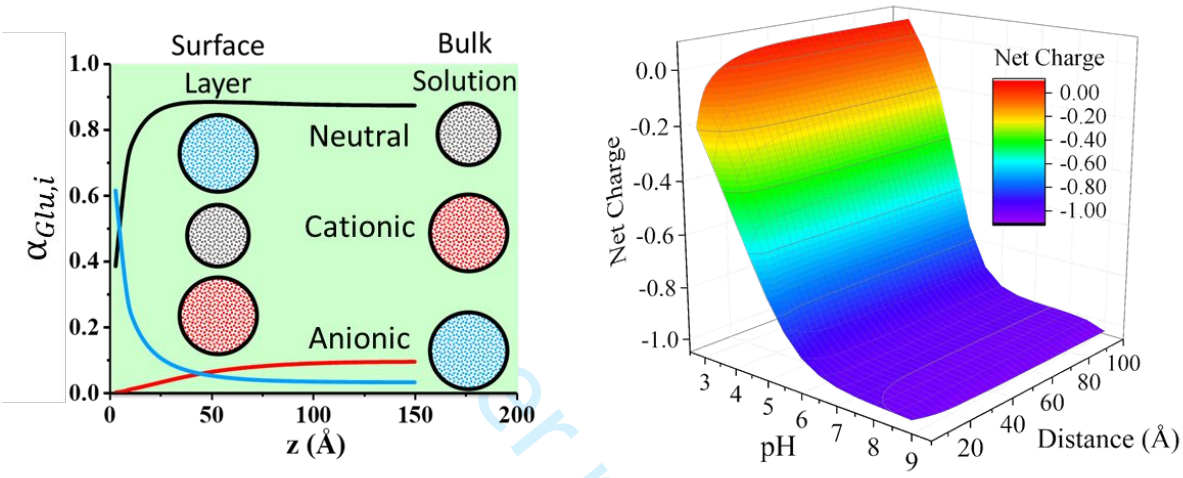

Figure 6. (a) The speciation of glutamic acid as a function of the distance from the surface at pH=3. (b) The net charge of the glutamic acid as a function of the distance from the surface and pH. In both cases, the total concentration of glutamic acid is 0.5 mM, and the NaCl concentration is 100 mM.

The presence of rutile, particularly when it is highly charged, leads to a significantly different speciation of the amino acid near the surface from that in the bulk solution. The variation in local ionization may span up to a few nanometers depending on the salt concentration. In Figure 6a, we present theoretical predictions for the speciation of glutamic acid as a function of the distance from the surface at pH=3.0. In this case, the rutile surface is positively charged as previously shown in Figure 3. The strong electrostatic attraction between the amino acid in the negatively charged state and the positively charged surface shifts the protonation equilibrium of the amino acid to the anionic state. Meanwhile, the amino acid in neutral and cationic states, which

dominate in the bulk solution, are depleted near the surface. While amino acids typically show monolayer adsorption and thus the long-range ionization behavior is of less significance, the strong variation in speciation near the surface results in drastic differences between the composition of the adsorbed layer and that in the bulk solution. On the other hand, the long-range ionization behavior may find more importance in the adsorption of polypeptides and proteins due to strong intrachain correlations.

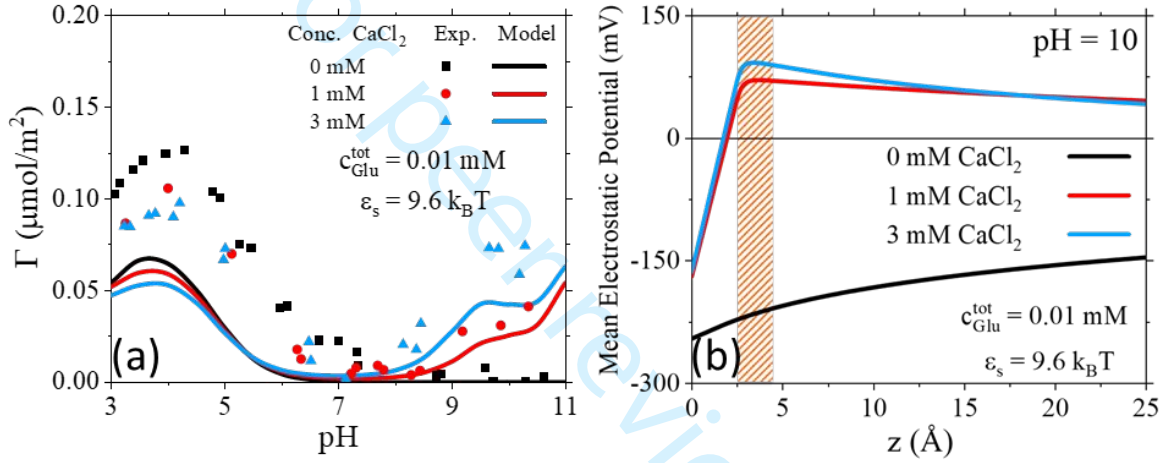

Figure 7. (a) The pH-dependent adsorption of glutamic acid on the rutile surface at different concentrations of $CaCl_2$ in 0.01 mM aqueous glutamic acid solution from experiment[36] (symbols) and the theoretical prediction (lines). (b) The mean electrostatic potential as a function of the distance from the rutile surface for the adsorption of glutamic acid at pH = 10 from salt-free and 1 or 3 mM $CaCl_2$ solutions. The shaded region corresponds to a monolayer of glutamic acid adsorbed at the surface.

We show in Figure 6b how the net charge of glutamic acid varies with the distance from the rutile surface and pH. In general, the net charge is shifted towards the charged state that favors interaction with the surface. At low pH, the glutamic acid has a positive net charge in the bulk solution while the rutile surface is also positively charged. In this case, the net charge is reduced

as the amino acid is positioned close to surface. The opposite occurs at high pH with the net charge increasing near the surface since rutile is negatively charged at these conditions. Again, an accurate description of the charge regulation for both the surface and amino acid is important to predict how changes in the environment affect the amino-acid adsorption.

Next, we consider the role of multivalent ions in facilitating the adsorption of amino acids. Because of electrostatic correlations, significant adsorption may take place in the presence of multivalent ions despite that the amino acid and the surface have the same sign of electric charge. Figure 7 shows the adsorption of glutamic acid at the rutile surface in a salt-free solution and two calcium chloride solutions of different concentrations. For both glutamic acid and calcium ions, the surface energy parameters are the same as those determined previously. For the salt-free case, glutamic acid exhibits a maximum adsorption at low pH with little to no adsorption when pH>7. Qualitatively, the pH effect is consistent with the adsorption at higher amino-acid concentrations as previously shown in Figure 4. The addition of calcium ions to the solution leads to significant adsorption of the glutamic acid at high pH when both the amino acid and the rutile surface are negatively charged.

To understand the origin of attraction, we show in Figure 7b the mean electrostatic potential as a function of the distance at pH=10 for the three aqueous solutions considered in Figure 7a. For the salt-free case (i.e., 0 mM $CaCl_2$), the mean electrostatic potential is strongly negative at the surface and decays slowly with the distance as predicted by a conventional electric double layer (EDL) model. However, in the presence of calcium ions, the surface potential is significantly reduced and the local electrostatic potential switches in sign (i.e., from negative to positive) signaling charge inversion. In other words, the surface charge is overcompensated by the oppositely charged ions through specific association and electrostatic correlations[41]. The charge

inversion leads to the adsorption of the negatively charged glutamic acid which experiences an effective attraction to the overcompensated "positive" surface despite itself being negatively charged. Although the agreement between experiment and theoretical predictions is only semi-quantitative, Figure 7 clearly demonstrates that our model captures the important physics regarding the effect of multivalent ions on the adsorption of amino acids at inorganic surfaces.

3.2 *Adsorption of basic amino acids*

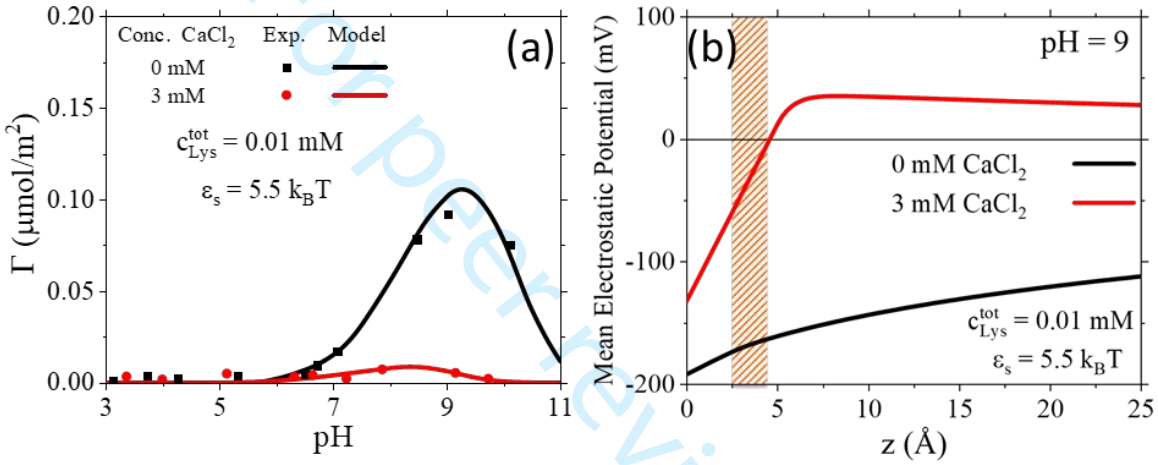

Figure 8. (a) The pH-dependent lysine adsorption at the rutile surface from experiment[36] (symbols) and the theoretical prediction (lines). (b) The mean electrostatic potential as a function of the distance from the rutile surface in two aqueous solutions at pH=9. Approximately, the shaded area corresponds to a monolayer of lysine at the rutile surface.

We now turn our attention to the adsorption of lysine, a basic amino acid, at the rutile surface. In the bulk solution, lysine molecules mostly exist in its positively charged state, except for high pH (i.e., pH>9) where its backbone amine group will deprotonate shifting the equilibrium to its neutral state. Further increase in the pH will result in the side-chain amine group also deprotonating and the anionic state of lysine becoming dominant. Figure 8 shows the adsorption of lysine at the rutile surface in a salt-free solution and that in a 3 mM calcium chloride solution.

While aspartic acid and glutamic acid display significant adsorption when they have the same electric charge as the surface, lysine shows no adsorption at similar conditions. Interestingly, no significant adsorption is observed even when the surface is neutral or weakly charged with a negative sign. The non-adsorption behavior can be attributed to the limited binding capability of its side chain with the rutile surface. In contrast to the carboxyl group in the side chain of aspartic or glutamic acid, there is less significant binding between the amine group in the lysine side chain with the hydroxyl groups from the rutile surface. In our coarse-grained model, the non-electrostatic effect is captured by a lower binding energy of each lysine molecule with the surface, ε_{surf} =5.5 k_BT, compared with 9.6 k_BT for the acidic amino acids. As a result, the electrostatic interactions play a more dominant role in lysine adsorption at the rutile surface.

When the solution pH is above the isoelectric point of the rutile surface (pI = 5.3), lysine molecules and the surface have opposite charges and the electrostatic attraction leads to strong adsorption of the amino acid. However, the adsorption shows a maximum at pH=9 beyond which it falls as a result of the increased prevalence of lysine molecules in the neutral state. The situation is similar to that found for acidic amino acids at low pH. In the presence of calcium ions, the adsorption of lysine drops dramatically compared to the salt-free case. This is not surprising because the divalent cations outcompete the monovalent lysine. As the non-electrostatic binding energy is relatively insignificant in comparison with that for acidic amino acids, lysine adsorption is more sensitive to the screening effects due to salt ions in the solution.

Figure 8b shows how the local electrostatic potential varies with the distance from the rutile surface. As discussed above, the presence of calcium ions leads to a significant reduction of the surface electric potential. The charge inversion hinders the adsorption of lysine molecules at the rutile surface even though the amino acid and the surface have opposite charges. The competition

in adsorption between the amino acid and the multivalent ions to the rutile surface is well captured by our coarse-grained model.

3.3 *Adsorption of neutral amino acids*

Lastly, we consider the adsorption of a neutral amino acid, dihydroxyphenylalanine (DOPA), to the rutile surface. From the practical perspective, understanding DOPA adsorption is highly important due to its extensive use in bioadhesive materials[42-44]. DOPA exhibits excellent adhesive and cohesive properties through its strong binding to inorganic surfaces by a bidentate bonding of its two hydroxyl groups in the side chain and complexation with multivalent ions by its aromatic group, respectively[45]. While most neutral amino acids show little or no adsorption at inorganic surfaces[18], DOPA displays strong adsorption that is highly dependent on the solution pH and salt concentration.

As demonstrated by spectroscopy measurements[46], DOPA binds with an inorganic surface in one of two configurations: lying flat or standing up. When a DOPA molecule is in its flat configuration, it interacts with the surface through its carboxyl group in the backbone and the two hydroxyl groups in its side chain. Meanwhile, the standing up orientation allows only for the interaction of the two hydroxyl groups with the surface. Since these configurations are dependent upon the availability of specific surface sites, the solution pH has noticeable effects on both the adsorption and configuration of DOPA due to the protonation or deprotonation of the surface sites.

In order to accurately describe the adsorption of DOPA to an inorganic surface, we must acknowledge the existence of these two orientations at the surface. Barhi et al. employed an extended triple layer model that describes DOPA attachment to the surface through either four or two surface sites[47]. The former corresponds to the lying flat orientation where the two phenolic oxygens and one of the carboxylate oxygens bind to the titanium atom on the surface while the

other carboxylate oxygen is hydrogen bonded to a hydroxyl group at the surface. On the other hand, the complexation with two surface sites involves one of the phenolic oxygens bonding to the titanium atom while the other phenolic oxygen is involved with hydrogen bonding to the surface. The surface complexation scheme can be described through the following chemical reactions[47]:

$$4-\mathrm{TiOH}+\mathrm{H_3DP}\leftrightarrow\left(-\mathrm{TiOH}\right)-\mathrm{Ti_3DP}+3\mathrm{H_2O} \tag{19}$$

$$2-\mathrm{TiOH}+\mathrm{H_3DP}\leftrightarrow\left(-\mathrm{TiOH_2^+}\right)-\mathrm{TiHDP^-}+\mathrm{H_2O} \tag{20}$$

where H_3DP represents DOPA in its neutral state. The thermodynamic equilibrium constants for these reactions can be related to the activities of the pertinent species by

$$K_{(-\mathrm{TiOH})-\mathrm{Ti_3DP}}=\frac{a_{(-\mathrm{TiOH})-\mathrm{Ti_3DP}}a_{\mathrm{H_2O}}^3}{a_{-\mathrm{TiOH}}^4 a_{\mathrm{H_3DP}}}\exp\left[\beta e\Delta\psi_{r,1}\right], \tag{21}$$

$$K_{\left(-\mathrm{TiOH_2^+}\right)-\mathrm{TiHDP^-}}=\frac{a_{\left(-\mathrm{TiOH_2^+}\right)-\mathrm{TiHDP^-}}a_{\mathrm{H_2O}}}{a_{-\mathrm{TiOH}}^2 a_{\mathrm{H_3DP}}}\exp\left[\beta e\Delta\psi_{r,2}\right]. \tag{22}$$

The inclusion of the exponential term results from the electrical work involved with moving ions and/or water dipoles to and from the surface[26]. The electrostatic work to displace water dipoles from the surface is given by $\Delta\psi_{\mathrm{H_2O}}=-n_{\mathrm{H_2O}}(\psi_s-\psi_\beta)$, where $n_{\mathrm{H_2O}}$ represents the stoichiometric coefficient of water molecules on the right-hand side of the reactions in Eqs. (19) and (20), ψ_s and ψ_β refer to the electric potentials at the surface and at the plane at which the DOPA molecule is adsorbed (i.e., when in contact with the surface, $z=\sigma_{DP}/2$). The electrical work involved in the first reaction is

$$\Delta\psi_{r,1}=3\psi_s-3\psi_\beta-3\left(\psi_s-\psi_\beta\right)=0 \tag{23}$$

where the three terms in the middle correspond to changes in the potentials experienced by the three H^+ ions adsorbing to the surface, the DP^{3-} ion adsorbing to the β-plane, and three H_2O

molecules desorbing from the surface, respectively. Thus, there is no contribution by the electrical work involved with moving ions and water molecules to and from the surface. On the other hand, the electrical work of the second reaction is

$$\Delta\psi_{r,2} = 2\psi_s - 2\psi_\beta - \left(\psi_s - \psi_\beta\right) = \psi_s - \psi_\beta \tag{24}$$

where the three terms in the middle correspond to changes in the electric potentials experienced by the two H^+ ions adsorbed at the surface, the HDP^{2-} ion adsorbed at the β-plane, and H_2O molecule desorbed from the surface, respectively. Based off the fitting with the experimental data, we determined the negative logarithmic equilibrium constants for the two reactions to be 11.6 and 5.8, respectively. The pK_a values are slightly different from those determined by Bahri et al. (11.8 and 6.4, respectively). The difference is expected because we consider thermodynamic non-ideality in addition to the direct Coulomb interactions.

We show in Figure 9a and b the adsorption of DOPA to the rutile surface versus the solution pH at different salt and total DOPA concentrations. The adsorption of most neutral amino acids shows little sensitivity to pH since they are not directly influenced by changes in the surface charge[48]. This is valid except at very low or high pH values when the ionized state of the amino acid becomes dominate. For example, a neutral amino acid typically carries a positive charge at pH<2 while the rutile surface is also positively charged. Similar to other neutral amino acids, the DOPA adsorption is reduced when the ionized states are favored at extreme pH values. However, DOPA adsorption varies with pH even though the molecule is entirely in its neutral state. Because of its association with the surface sites (i.e., TiOH), the surface sites in protonated ($TiOH_2^+$) or deprotonated (TiO^-) states will impact DOPA adsorption.

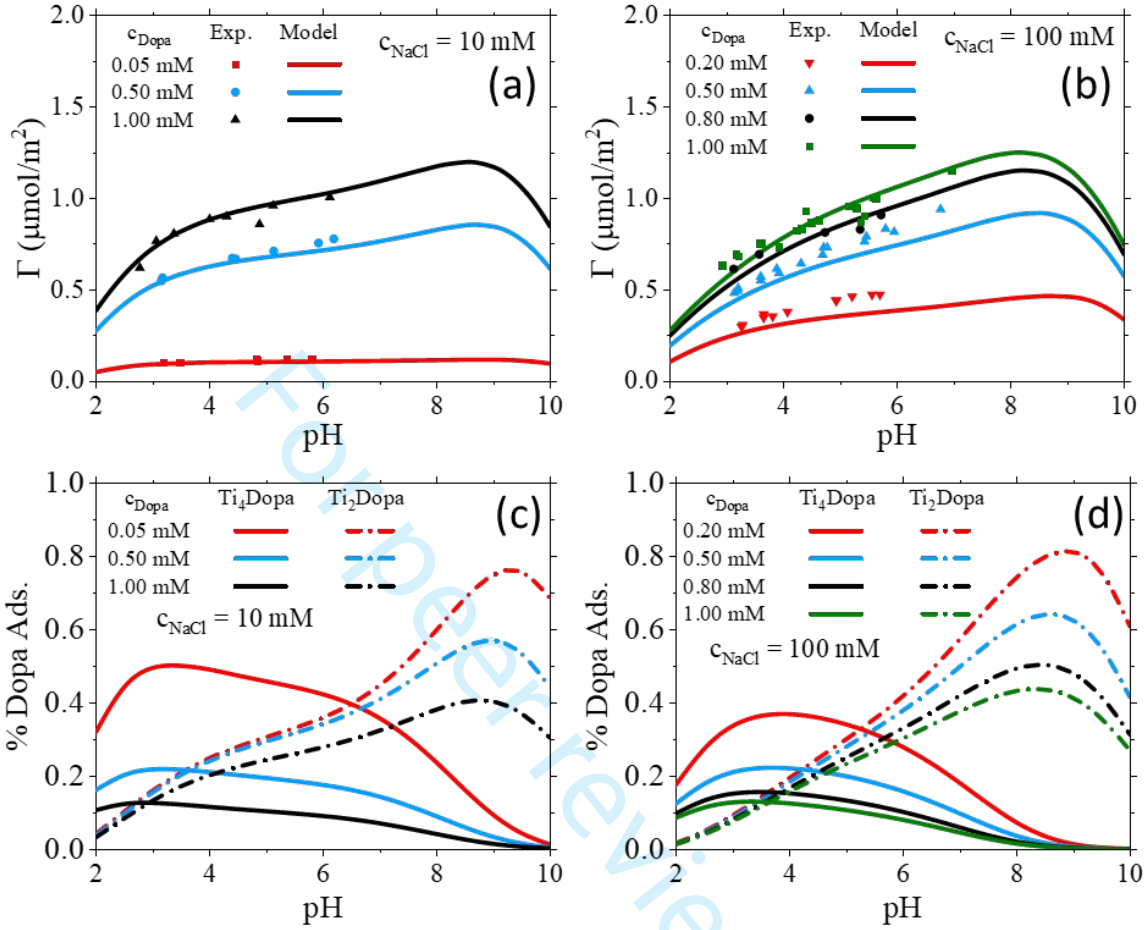

Figure 9. The adsorption of dihydroxyphenylalanine (DOPA) at the rutile surface versus pH in (a) 10 mM and (b) 100 mM NaCl solutions. Different lines are theoretical predictions corresponding to various total DOPA concentrations, the symbols are from experiment[47]. The speciation of DOPA at the rutile surface as a function of pH predicted according to the thermodynamic model. Ti_nDOPA refers to the binding of DOPA to *n* titanium surface sites as given by Eqs. (21) and (22).

To understand further why DOPA adsorption increases as the pH rises, we may consider the distribution of adsorbed DOPA according to the surface configurations:

$$n_{DP}^{ads} = n_{(>\mathrm{TiOH})>\mathrm{Ti_3DP}} + n_{(>\mathrm{TiOH_2^+})>\mathrm{TiHDP^-}}. \quad (25)$$

Based off the conditions of chemical equilibrium as shown in Eqs. (21) and (22), we may relate the surface concentrations of DOPA in different configurations to the number density of surface hydroxyl groups:

$$n_{DP}^{ads} = \mathrm{K}_1' n_{\mathrm{TiOH}}^4 c_{\mathrm{DP}} + \mathrm{K}_2' \exp\left[-\beta e \Delta\psi_{r,2}\right] n_{\mathrm{TiOH}}^2 c_{DP} \tag{26}$$

where indices 1 and 2 refer to the chemical reactions involving four and two surface sites, respectively, and the primes denote the apparent equilibrium constants, i.e., after the conversions from activity to the number density or concentration. Eq. (26) indicates that DOPA adsorption is intrinsically related to the availability of surface hydroxyl sites and the DOPA concentration at the surface. As the number density of surface hydroxyl sites decreases as the pH deviates from the isoelectric point, we expect that the DOPA adsorption will be maximized near the isoelectric point. Meanwhile, the exponential factor in the second term on the right side of Eq. (26) explains why DOPA adsorption increases with pH beyond the isoelectric point. When the surface is positively charged, $\Delta\psi_{r,2}$ is greater than zero; and it is less than zero when the surface is negatively charged, i.e., the surface potential is always greater in magnitude than that at the adsorption plane of DOPA. Because the magnitude of $\Delta\psi_{r,2}$ increases as the pH deviates more from the isoelectric point, the exponential term approaches unity from below as the pH increases towards the isoelectric point. Further increase in the pH will increase the absolute value of the exponential factor and thus improve the adsorption of DOPA. Therefore, we conclude that the increase in DOPA adsorption with pH results from the favorable electrostatic work due to the complexation of the DOPA molecule with the surface. The importance of electrostatic interactions in the binding of a neutral DOPA molecule with the rutile surface explains why the salt concentration plays a significant role in the adsorption.

Figure 9c and d present the fraction of DOPA in two surface configurations. The electrostatic work is a contributing factor for DOPA transition from lying flat to standing up as the pH rises. The increase in salt concentration tends to shift the transition between the two surface configurations to a lower pH due to electrostatic screening. Another major factor in determining the surface configuration of DOPA is its local number density. When the surface concentration of DOPA increases, it lowers the pH at which the transition takes place due to the competition of DOPA molecules with each other at the surface. At small surface concentrations, the competition for the surface sites is less important, which explains why the DOPA molecules are mostly lying flat at the surface. Clearly, the surface complexation model provides a satisfactory description of DOPA adsorption to the titanium surface and valuable insight into the mechanisms of DOPA attachment to inorganic surfaces in an aqueous solution.

4. Conclusion

There have been substantial interests in understanding the interaction of polypeptides and proteins with inorganic surfaces due to their applications to the design of bioadhesives and the remediation of biofouling. In the present study, we have initiated a theoretical work for such possibilities by employing a coarse-grained model for amino acids that captures their adsorption at an inorganic surface under different solution conditions. By leveraging our previous work to account for the key physics governing charge regulation and the interaction of amino acids with ionic species in aqueous solutions, we developed a molecular-thermodynamic framework that is able to predict the adsorption of amino acids on inorganic surfaces driven by either electrostatic binding or surface complexation. The thermodynamic model integrates ionization equilibrium for both amino acids and inorganic surfaces with the classical density functional theory (cDFT) that facilitates an accurate description of the inhomogeneous distributions of amino acids and ionic

species near inorganic surfaces. Importantly, this model accounts for both chemical and physical interactions between amino acids and an inorganic surface, which is key to capturing the changes in adsorption due to variation in solution conditions.

To demonstrate the effectiveness of this molecular thermodynamic model, we compare theoretical predictions directly with experimental adsorption data for different charge types (i.e., acidic, basic, and neutral) of amino acids on a rutile surface. We first showed that the deprotonation and protonation of hydroxyl sites at the inorganic surface can be well described by coupling the chemical equilibrium of the surface sites with cDFT calculation for ion distributions. We then investigated the adsorption behavior of different amino acids at the rutile surface in aqueous solutions that are varied in pH, amino acid concentration, salt type and concentration. We found that amino-acid adsorption typically shows a maximum an intermediate pH value that is dependent upon the salt type and concentration. While the increase in salt concentration promotes the ionization of the surface sites, it also weakens the electrostatic interaction between amino acid and the surface. Therefore, the addition of salt reduces the adsorption of amino acid and shifts the pH to a higher value where the maximum adsorption takes place. For acidic amino acids, the non-electrostatic surface binding makes a significant contribution to the adsorption even when the electrostatic charges of the amino acid and the surface are of the same sign. On the other hand, a basic amino acid like lysine shows much weaker dependence on non-electrostatic surface binding and the adsorption is mostly driven by electrostatic attraction from the surface. A maximum adsorption takes place at high pH when the amino acid and surface are oppositely charged. Lastly, we considered the adsorption of DOPA, a neutral amino acid, to the rutile surface through a combination with the surface complexation model that accounts for the two configurations of DOPA molecules at the rutile surface.

An accurate description of the charge regulation for both amino acids and the underlying surface in a highly inhomogeneous environment plays an important role in understanding the adsorption behavior of amino acids, particularly the acidic and basic amino acids, to inorganic surfaces. The interaction between amino acids and the surface also affects equilibrium between different charged states leading to the speciation amino acid molecules significantly different from that in the bulk solution. Because of the shift in speciation, the amino acids adsorbed at a highly charged surface may exist in an ionized state of opposite charge of the surface while those in the bulk solution are entirely neutral. Although the molecular-thermodynamic model employs a number of semi-empirical parameters, it provides a predictive description of thermodynamic non-idealities that are relevant to describe the environmental effects on both amino-acid adsorption and chemical equilibrium. In the future, we plan to extend this molecular-thermodynamic framework to describing the adsorption of polypeptides and flexible proteins which are of keen interest for practical applications.

Acknowledgements

This work is supported by the National Science Foundation Harnessing the Data Revolution Big Idea under Grant No. NSF 1940118. Additional support is provided by the National Science Foundation Graduate Research Fellowship under Grant No. DGE-1326120. The computational work used resources of the National Energy Research Scientific Computing Center (NERSC), a DOE Office of Science User Facility supported by the Office of Science of the U.S. Department of Energy, under Contract DE-AC02-05CH11231.

Data Sharing and Data Availability: The data that support the findings of this study are available from the corresponding author upon reasonable request.

References:

1. Balkenende DWR, Winkler SM, Messersmith PB. Marine-inspired polymers in medical adhesion. *European Polymer Journal.* 2019;116:134-143.
2. Adamczyk Z. Protein adsorption: A quest for a universal mechanism. *Current Opinion in Colloid & Interface Science.* 2019;41:50-65.
3. Mahmoudi M. Debugging Nano–Bio Interfaces: Systematic Strategies to Accelerate Clinical Translation of Nanotechnologies. *Trends in Biotechnology.* 2018;36(8):755-769.
4. Schwaminger S, Blank-Shim SA, Borkowska-Panek M, et al. Experimental characterization and simulation of amino acid and peptide interactions with inorganic materials. *Eng Life Sci.* 2018;18(2):84-100.
5. Costa D, Savio L, Pradier CM. Adsorption of Amino Acids and Peptides on Metal and Oxide Surfaces in Water Environment: A Synthetic and Prospective Review. *The Journal of Physical Chemistry B.* 2016;120(29):7039-7052.
6. Kitadai N, Yokoyama T, Nakashima S. ATR-IR spectroscopic study of L-lysine adsorption on amorphous silica. *Journal of Colloid and Interface Science.* 2009;329(1):31-37.
7. Lambert JF. Adsorption and polymerization of amino acids on mineral surfaces: a review. *Orig Life Evol Biosph.* 2008;38(3):211-242.
8. Shchelokov A, Palko N, Potemkin V, et al. Adsorption of Native Amino Acids on Nanocrystalline TiO2: Physical Chemistry, QSPR, and Theoretical Modeling. *Langmuir.* 2019;35(2):538-550.
9. Greiner E, Kumar K, Sumit M, et al. Adsorption of l-glutamic acid and l-aspartic acid to γ-Al2O3. *Geochimica et Cosmochimica Acta.* 2014;133:142-155.
10. Begonja S, Rodenas LAG, Borghi EB, Morando PJ. Adsorption of cysteine on TiO2 at different pH values: Surface complexes characterization by FTIR-ATR and Langmuir isotherms analysis. *Colloids and Surfaces A: Physicochemical and Engineering Aspects.* 2012;403:114-120.
11. El Shafei GMS, Moussa NA. Adsorption of Some Essential Amino Acids on Hydroxyapatite. *Journal of Colloid and Interface Science.* 2001;238(1):160-166.
12. Imamura K, Mimura T, Okamoto M, Sakiyama T, Nakanishi K. Adsorption Behavior of Amino Acids on a Stainless Steel Surface. *Journal of Colloid and Interface Science.* 2000;229(1):237-246.
13. O'Connor AJ, Hokura A, Kisler JM, Shimazu S, Stevens GW, Komatsu Y. Amino acid adsorption onto mesoporous silica molecular sieves. *Separation and Purification Technology.* 2006;48(2):197-201.
14. Horányi G. Adsorption of primary amino compounds at platinum electrodes: A survey of radiotracer studies. *Electrochimica Acta.* 1990;35(6):919-928.
15. Hughes ZE, Walsh TR. What makes a good graphene-binding peptide? Adsorption of amino acids and peptides at aqueous graphene interfaces. *Journal of Materials Chemistry B.* 2015;3(16):3211-3221.
16. Dasetty S, Barrows JK, Sarupria S. Adsorption of amino acids on graphene: assessment of current force fields. *Soft Matter.* 2019;15(11):2359-2372.
17. Hoefling M, Iori F, Corni S, Gottschalk KE. Interaction of amino acids with the Au(111) surface: adsorption free energies from molecular dynamics simulations. *Langmuir.* 2010;26(11):8347-8351.

18. Vlasova N, Golovkova L. The adsorption of amino acids on the surface of highly dispersed silica. *Colloid J+.* 2004;66(6):657-662.
19. Jonsson CM, Jonsson CL, Sverjensky DA, Cleaves HJ, Hazen RM. Attachment of l-Glutamate to Rutile (α-TiO2): A Potentiometric, Adsorption, and Surface Complexation Study. *Langmuir.* 2009;25(20):12127-12135.
20. Jonsson CM, Jonsson CL, Estrada C, Sverjensky DA, Cleaves HJ, Hazen RM. Adsorption of l-aspartate to rutile (α-TiO2): Experimental and theoretical surface complexation studies. *Geochimica et Cosmochimica Acta.* 2010;74(8):2356-2367.
21. Gallegos A, Wu J. Charge Regulation of Natural Amino Acids in Aqueous Solutions. *Journal of Chemical & Engineering Data.* 2020;65(12):5630-5642.
22. Kong X, Jiang J, Lu D, Liu Z, Wu J. Molecular Theory for Electrokinetic Transport in pH-Regulated Nanochannels. *The Journal of Physical Chemistry Letters.* 2014;5(17):3015-3020.
23. Ong GMC, Gallegos A, Wu J. Modeling Surface Charge Regulation of Colloidal Particles in Aqueous Solutions. *Langmuir.* 2020;36(40):11918-11928.
24. Yang J, Su H, Lian C, Shang Y, Liu H, Wu J. Understanding surface charge regulation in silica nanopores. *Physical Chemistry Chemical Physics.* 2020;22(27):15373-15380.
25. Sverjensky DA, Fukushi K. A predictive model (ETLM) for As(III) adsorption and surface speciation on oxides consistent with spectroscopic data. *Geochimica et Cosmochimica Acta.* 2006;70(15):3778-3802.
26. Sverjensky DA, Fukushi K. Anion Adsorption on Oxide Surfaces: Inclusion of the Water Dipole in Modeling the Electrostatics of Ligand Exchange. *Environmental Science & Technology.* 2006;40(1):263-271.
27. Tamura H, Mita K, Tanaka A, Ito M. Mechanism of Hydroxylation of Metal Oxide Surfaces. *Journal of Colloid and Interface Science.* 2001;243(1):202-207.
28. Akratopulu KC, Kordulis C, Lycourghiotis A. Effect of temperature on the point of zero charge and surface charge of TiO2. *Journal of the Chemical Society, Faraday Transactions.* 1990;86(20):3437-3440.
29. Loux NT. Extending the diffuse layer model of surface acidity behaviour: III. Estimating bound site activity coefficients. *Chemical Speciation & Bioavailability.* 2009;21(4):233-244.
30. Gómez-Bombarelli R, González-Pérez M, Pérez-Prior MT, Calle E, Casado J. Computational Calculation of Equilibrium Constants: Addition to Carbonyl Compounds. *The Journal of Physical Chemistry A.* 2009;113(42):11423-11428.
31. Mansoori GA, Carnahan NF, Starling KE, Leland TW. Equilibrium Thermodynamic Properties of the Mixture of Hard Spheres. *The Journal of Chemical Physics.* 1971;54(4):1523-1525.
32. Maribo-Mogensen B, Kontogeorgis GM, Thomsen K. Comparison of the Debye–Hückel and the Mean Spherical Approximation Theories for Electrolyte Solutions. *Industrial & Engineering Chemistry Research.* 2012;51(14):5353-5363.
33. Jin Z, Tang Y, Wu J. A perturbative density functional theory for square-well fluids. *The Journal of Chemical Physics.* 2011;134(17):174702.
34. Jang HM, Fuerstenau DW. The specific adsorption of alkaline-earth cations at the rutile/water interface. *Colloids and Surfaces.* 1986;21:235-257.
35. Kosmulski M. Isoelectric points and points of zero charge of metal (hydr)oxides: 50years after Parks' review. *Advances in Colloid and Interface Science.* 2016;238:1-61.

36. Lee N, Sverjensky DA, Hazen RM. Cooperative and Competitive Adsorption of Amino Acids with Ca2+ on Rutile (α-TiO2). *Environmental Science & Technology.* 2014;48(16):9358-9365.
37. Misra RP, de Souza JP, Blankschtein D, Bazant MZ. Theory of Surface Forces in Multivalent Electrolytes. *Langmuir.* 2019;35(35):11550-11565.
38. Imamura K, Kawasaki Y, Awadzu T, Sakiyama T, Nakanishi K. Contribution of acidic amino residues to the adsorption of peptides onto a stainless steel surface. *Journal of Colloid and Interface Science.* 2003;267(2):294-301.
39. Nagayasu T, Yoshioka C, Imamura K, Nakanishi K. Effects of carboxyl groups on the adsorption behavior of low-molecular-weight substances on a stainless steel surface. *Journal of Colloid and Interface Science.* 2004;279(2):296-306.
40. De Stefano C, Foti C, Gianguzza A, Sammartano S. The interaction of amino acids with the major constituents of natural waters at different ionic strengths. *Marine Chemistry.* 2000;72(1):61-76.
41. de Vos WM, Lindhoud S. Overcharging and charge inversion: Finding the correct explanation(s). *Advances in Colloid and Interface Science.* 2019;274:102040.
42. Waite JH. Mussel adhesion – essential footwork. *The Journal of Experimental Biology.* 2017;220(4):517.
43. Stewart RJ, Ransom TC, Hlady V. Natural underwater adhesives. *Journal of Polymer Science Part B: Polymer Physics.* 2011;49(11):757-771.
44. Kord Forooshani P, Lee BP. Recent approaches in designing bioadhesive materials inspired by mussel adhesive protein. *Journal of polymer science Part A, Polymer chemistry.* 2017;55(1):9-33.
45. Moulay S. Recent Trends in Mussel-Inspired Catechol-Containing Polymers. Part 1 (A Review. 2018.
46. Gulley-Stahl H, Hogan PA, Schmidt WL, Wall SJ, Buhrlage A, Bullen HA. Surface complexation of catechol to metal oxides: an ATR-FTIR, adsorption, and dissolution study. *Environmental science & technology.* 2010;44(11):4116-4121.
47. Bahri S, Jonsson CM, Jonsson CL, Azzolini D, Sverjensky DA, Hazen RM. Adsorption and Surface Complexation Study of L-DOPA on Rutile (α-TiO2) in NaCl Solutions. *Environmental Science & Technology.* 2011;45(9):3959-3966.
48. Krohn JE, Tsapatsis M. Phenylalanine and Arginine Adsorption in Zeolites X, Y, and β. *Langmuir.* 2006;22(22):9350-9356.